

The effects of deep brain stimulation in neuropathic pain induced rats

Jaehyung Kim

Department of Medical Science

The Graduate School, Yonsei University

The effects of deep brain stimulation in neuropathic pain induced rats

Jaehyung Kim

Department of Medical Science

The Graduate School, Yonsei University

The effects of deep brain stimulation in neuropathic pain induced rats

Directed by Professor Jin Woo Chang

The Doctoral Dissertation submitted to the
Department of Medical Science, the Graduate School
of Yonsei University in partial fulfillment of the
requirements for the degree of Doctor of Philosophy
of Medical Science

Jaehyung Kim

June 2010

This certifies that the Doctoral Dissertation of
Jaehyung Kim is approved.

Thesis Supervisor: Jin Woo Chang

Thesis Committee Member 1: Taick Sang Nam

Thesis Committee Member 2: Kyung Ah Park

Thesis Committee Member 3: Kyung Tae Min

Thesis Committee Member 4: Bae Hwan Lee

The Graduate School

Yonsei University

June 2010

Acknowledgements

The time of my doctor degree has passed so fast and now when I look back my last 4 years, only regrets and longing have remained.

I would like to appreciate sincerely to those who helped and gave encouragements to me to finish all processes successfully even in those hard and eventful times.

First of all, I would like to appreciate to academic advisor Jin Woo Chang, M.D., Ph.D. for having taken care of me with love and concern during whole 4 years even in his busy schedule. And also, truly appreciate to professor Taick Sang Nam, M.D., Ph.D., professor Kyung Ah Park, M.D., Ph.D., professor Kyung Tae Min, M.D., Ph.D., and professor Bae Hwan Lee, Ph.D. for gave this thesis infinite advises and bright teachings.

I am deeply thankful to my father and mother for their great love and assiduous care during my whole life. Because I know that I cannot even exist without my parent's great love, I am thankful to them again and again. Also, thankful to my brother Sung Min who always gave me his faith and support.

In addition, I am thankful to my father-in-law, mother-in-law, and sister-in-law who give me great concerns as strong supporter as well.

I would like to have all this glory forever with my wife Ji Young who always covers me with bright smile and love whenever I felt tired with study and works.

I am thankful to all the members of my laboratory family Yong Sup Ph.D., Da Un, Dongkyu and Jinhyung. And also, thankful to Jin Hwan, Kyou sik, Sung Eun, and Se-Ik Park, Ph.D. those who gave me great help to finish this thesis. In addition, I am really appreciate to Yoon Hee Cho, Ph.D. and Hyun Jung Lee. And also want to share this pleasure with Jin Soo, Sung Soo, Sung Young, Young Suk Park, M.D., Won Suk Chang, M.D., Joo Pyung Kim, M.D., and Eun Jung Kwan who always encouraged me.

Lastly, sincerely thankful to Jesus Christ for go with me always and saving me from sins. Thankful to acknowledge me that I cannot accomplish anything without his loves and cares.

I am truly appreciate that all the experiences from my last 4 years had been precious foundation for my next step and thankful to all people who gave me the chance to have this great experiences and dedicate this thesis to them.

June 2010

Jaehyung Kim

TABLE OF CONTENTS

ABSTRACT	1
I. INTRODUCTION	3
II. MATERIALS AND METHODS	
1. Neuropathic pain rat model	6
A. Animals	6
B. Induction of neuropathic pain	6
2. Deep brain stimulation of rats	7
A. Anchor system	7
B. Stimulation electrode	8
C. Deep brain stimulator	8
D. Stereotaxic implantation of electrode into the target sites and stimulation	9
3. Micro-PET imaging	10
A. ¹⁸ F-FDG and micro-PET scanning	10
B. Analysis of imaging	10
4. Analysis of the analgesic effect of high-frequency DBS on neuropathic pain rats	12

A. Behavior tests	12
B. Immunohistochemistry	13
C. Western blot	14
5. Verification of the analgesic effect by introducing GAD65 into the spinal dorsal horn	15
A. Preparation of the rAAV2-GAD65	15
B. rAAVs injection in rats	16
C. Microdialysis	17
D. HPLC analysis	18
6. Statistical analysis	18

III. RESULTS

1. Induced neuropathic pain on rats	19
2. Micro-PET scan of neuropathic pain rat models	21
3. Verification of the DBS electrode insertion effects	22
4. Effect of high-frequency DBS according to target site	24
A. ACC	24
B. PAG	26
C. VPM	27
D. VPL	28

5. Effect of DBS on c-fos, GAD65, and parvalbumin expression in brain and spinal dorsal horn	29
A. Effect of VPL-DBS in neuropathic pain rat	29
B. Change of c-fos expression in the rat brain	31
C. GAD65 immunoreactivity in spinal dorsal horn	32
D. Parvalbumin expression in spinal dorsal horn	33
6. Verification of analgesic effects by introducing GAD65 <i>in vivo</i>	35
A. rAAV expression GAD65 gene <i>in vitro</i>	35
B. Injection of rAAV into the sciatic nerve efficiently transduced DRG in neuropathic pain rats	37
C. GAD65 can be detected by rAAV2-GAD65 injection into the sciatic nerve	39
D. Injection of rAAV2-GAD65 into the sciatic nerve produces GAD65 <i>in vivo</i> , induced by GABA increase in the spinal dorsal horn	40
E. Injection of rAAV2-GAD65 reduces mechanical allodynia in neuropathic pain rat model	43
F. GAD65 reduces c-fos like immunoreactivity in spinal dorsal horn	45

IV. DISCUSSION	47
V. CONCLUSION	56
REFERENCES	57
ABSTRACT (IN KOREA)	68

LIST OF FIGURES

Figure 1. Neuropathic pain in rats	7
Figure 2. Comparison of behavior tests scores between neuropathic pain and naïve groups after sciatic nerve injury	20
Figure 3. Activated and deactivated brain structures of neuropathic pain on rats	22
Figure 4. Withdrawal foot lift frequency at pre- and post-operation in DBS electrode implant groups	23
Figure 5. Target site of ACC and withdrawal foot-lift frequency for <i>von Frey</i> tests in neuropathic pain-DBS rats	25
Figure 6. Behavior tests of mechanical and thermal allodynia for PAG-DBS in neuropathic pain rats before and after stimulation	26
Figure 7. Mechanical and thermal allodynia before and after VPM-DBS in neuropathic pain rats	27
Figure 8. Mechanical and thermal allodynia before and after	

VPL- DBS in neuropathic pain rats	28
Figure 9. Mechanical allodynia of VPL-DBS	30
Figure 10. c-fos like immunoactivity in neurons of the spinal dorsal horn in ipsilateral side	31
Figure 11. Comparison of c-fos expression	32
Figure 12. GAD65 expression in the ipsilateral spinal dorsal horn.	33
Figure 13. Parvalbumin expression in the spinal dorsal horn in neuropathic pain rats	34
Figure 14. Schematic illustration of rAAV2 vectors and endogenous GAD65 expression in HeLa cells after transduction with rAAV vectors	36
Figure 15. Detection of GAD65 and GABA expression ...	37
Figure 16. rAAV2-mediated transgene expression in DRG	38
Figure 17. Expression of GAD65 in DRG	40
Figure 18. GAD expression in the spinal dorsal horn	42
Figure 19. GABA secretion in the spinal dorsal horn	42

Figure 20. Therapeutic effects of sciatic nerve-administered rAAV2-GAD65 determined by behavior examination	44
Figure 21. c-fos detection in the ipsilateral spinal dorsal horn	46
Figure 22. Activation of brain sites with mechanical and cold stimuli to neuropathic pain	49
Figure 23. Molecular changes in the central and peripheral nervous system with VPL-DBS in the neuropathic pain rat model	53
Figure 24. Descending modulation with VPL-DBS in the neuropathic pain rat model	54
Figure 25. Hypothesis of descending modulation with VPL-DBS in the peripheral nervous system of the neuropathic pain rat model	55

<ABSTRACT>

The effects of deep brain stimulation in neuropathic pain induced rats

Jaehyung Kim

Department of Medical Science

The Graduate School, Yonsei University

(Directed by Professor Jin Woo Chang)

Neuropathic pain induced by peripheral nerve injury is clinically very common. High-frequency deep brain stimulation (DBS) is an effective treatment for chronic neuropathic pain, but the mechanisms underlying its analgesic effects are not precisely known. I investigated the mechanism of high-frequency DBS-related analgesia on neuropathic symptoms using male Sprague-Dawley rats with peripheral nerve injuries to induce neuropathic pain.

Rats were divided into four groups, naïve, naïve + VPL-DBS, neuropathic pain, and neuropathic pain + VPL-DBS. Before and after VPL-DBS, c-fos and GAD65 in the prefrontal cortex, thalamus, and spinal dorsal horn were measured by western blot. In the neuropathic pain + VPL-DBS group, an analgesic effect was observed compared to the neuropathic pain group, and significant c-fos expressions was seen after VPL-DBS in the prefrontal cortex and thalamus. Also, the expressions of GAD65 in the neuropathic pain + VPL-DBS group was slightly higher in the spinal dorsal horn than in the neuropathic pain group, while c-fos expression was decreased. These results suggested that VPL-DBS exerts an effect at both the brain and spinal cord level. High-frequency DBS suppressed the hyper-excited neuronal activities, especially in the prefrontal cortex and thalamus area, and modulate the pain threshold by upregulation of GAD65 expression in spinal dorsal horn.

Key words: neuropathic pain, high-frequency deep brain stimulation(DBS), ventral posterolateral thalamic nucleus(VPL), glutamic acid decarboxylase(GAD), c-fos

The effects of deep brain stimulation in neuropathic pain induced rats

Jaehyung Kim

Department of Medical Science
The Graduate School, Yonsei University

(Directed by Professor Jin Woo Chang)

I. INTRODUCTION

Pain is divided into two major types; adoptive pain and neuropathic pain¹. Adoptive pain has an important physiological function in survival. However, neuropathic pain occurs only after nerve damage, and does not result from the

repetitive applications of adoptive pain. Long-term changes both in the peripheral and central nervous system are likely to occur after nerve damage². Consequently, the pain sensation might be significantly amplified, or non-noxious stimuli may give rise to pain because of long-term plastic changes in the injured or injury-related area^{3,4}. Neuropathic pain is likely to be associated with long-term plastic changes along the somatosensory pathway from the peripheral to the central nervous system. Therefore, neuropathic pain is difficult to cure with available medical treatment⁵.

Recently, a lot of progresses has been seen in medical and surgical modalities for treating chronic pain⁶⁻⁹. However, many neuropathic pain patients respond ineffectively to currently available medicines^{10,11}. Also lesioning brain structures may accompany some side effects. Recently, neurosurgeons have developed the deep brain stimulation (DBS) technique, a fascinateive strategy that has been considered in neurodegenerative diseases such as Parkinson's disease and neuropathic pain^{8,12-15}. DBS is a minimally invasive alternative to drug treatment for painful conditions¹⁶. Some studies have demonstrated that high-frequency electrical stimulation of the nervous system can inhibit pain signal transmissions¹⁷. Although the mechanism by which high-frequency DBS works is still not known, DBS has been shown to have an analgesic effect on neuropathic pain^{13,18}.

According to current knowledge, pain signal starts from a peripheral nerve and moves to the somatosensory cortex through the rostral ventromedial medulla (RVM), periaqueductal gray (PAG), hypothalamus, frontal lobe, amygdala, primary somatosensory cortex, and anterior cingulate cortex (ACC)^{13,19-22}. When neuropathic pain occurs, brain regions differ in activity^{1,23-25}. When high-frequency DBS to PAG, VPL, or ACC regions is clinically applied, changes in brain activities occur during the neuropathic pain stage^{8,26}. These changes in brain activities with high-frequency DBS have the effect of reducing pain^{18,27}. High-frequency DBS is known to be an effective treatment for neuropathic pain but generally it is the result of experiences and no defined mechanism had been known to date.

Therefore, the aim of this study was to determine the effect of high-frequency DBS analgesic effects, using stimulation electrodes and stimulators to generate neuropathic pain rats. The stimulation electrode and stimulator were particularly designed for animal experimentation. I also used a small electrode fixation structure that was useful for investigating behavior changes after high-frequency DBS.

II. MATERIALS AND METHODS

1. Neuropathic pain rat model

A. Animals

This study was conducted according to the guidelines of the Ethical Committee of International Association for the Study of Pain and the American Association for the Accreditation of Laboratory Animal Care²⁸. Male Sprague-Dawley rats were housed in groups of three per cage during the experimental period with free access to feed and water. Rats were kept in a temperature- and humidity-controlled room with a 12-hour light/dark cycle. The rats weighing 180 - 200 g were used.

B. Induction of neuropathic pain

Under pentobarbital sodium (50 mg / kg, i.p. injection) anesthesia, a segment of the left sciatic nerve was exposed at the mid-thigh level. Surrounding tissues were carefully removed and the sciatic nerve was gently held in place with forceps. Three major divisions of the sciatic nerve (tibial, sural and common peroneal nerves) were clearly separated under a surgical microscope (Olympus, Japan)(Figure 1). To generate an

efficient neuropathic pain model, the tibial and sural nerves were tightly ligated and completely transected and the common peroneal nerve was left intact²⁹. Hemostasis was completed and the cut was closed with muscle and skin sutures.

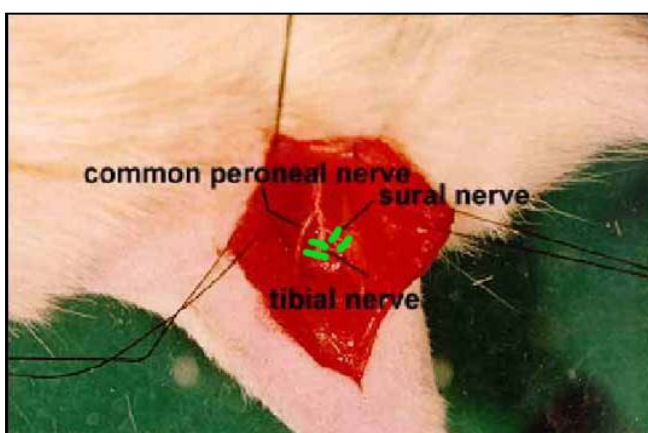


Figure 1. Neuropathic pain in rats. Tibial and sural nerves, the major branch of the sciatic nerve, were tightly ligated and transected, while the common peroneal nerve was left intact.

2. Deep brain stimulation of rats

A. Anchor system

A unique, newly designed anchor fixed the stimulation electrode into the

rat brain. The anchor was made of biocompatible teflon to minimize infections and inflammation. The anchor firmly fixed the stimulation electrode with glue (Elmer, USA) on the skull surface³⁰ and helped the scalp to close easily, and reduced the scar size after implantation of the stimulation electrodes. This allowed the stable, long-term maintenance of the experimental conditions.

B. Stimulation electrode

Tungsten stimulation electrodes (diameter 200 μm , 5 μm parylene coating) were inserted into the target site. The tip of electrode was tapered by electro-chemical etching to reduce the lesion effect of the target area³¹. The tapered length of the electrode was 2 mm and the area of the stimulation site was about 0.035 m^2 . The impedance of the electrode was $15 \pm 1 \text{ k}\Omega$ in saline and 1 kHz with a potentiostat (IM6e, Zahner Elektrik, Germany).

C. Deep brain stimulator

A newly developed, small-size stimulator was used to generate current stimulus pulses. A neural stimulation system was developed to control neural signals in neural circuitries in the central or peripheral nervous

system. It consisted of logical blocks that allowed setting various stimulation parameters and electrodes to interface with the neural cells.

D. Stereotaxic implantation of electrode into the target sites and stimulation

Two weeks after the completion of the surgical neuropathic pain model, an electrode was implanted into the target site in the DBS group. It was unilaterally implanted into selected animals with a teflon anchor at each target site at stereotactic coordinates according to the stereotactic atlas of Paxinos and Watson³². The coordinated target sites were ACC (anteroposterior, AP: 1 mm forward of bregma; mediolateral, ML: 0.5 mm right side of bregma, dorsoventral, DV: -2.5 mm below of dura), PAG (AP: -5 mm behind the bregma, ML: 0.4 mm right side of bregma, DV: -6.0 mm below the dura), ventral posteromedial thalamic nucleus (VPM; AP : -3.4 mm behind the bregma, ML : 2.4 mm right side of bregma, DV : -6.4 mm below the dura), and ventral posterolateral thalamic nucleus (VPL; AP : -2.2 mm behind the bregma, ML : 2.8 mm right side of bregma, DV : -6.0 mm below the dura). Electrodes were firmly secured with glue³⁰. Stimulation electrodes and current stimulators were connected by a multi-stranded extension cable. Voltages for stimulation parameters ranged from

0 to 5 v, and the pulse rate (130 Hz) and duration (60 μ s) were fixed. Parameters were monitored in real-time during the entire stimulation period with an oscilloscope (HDS1022M, Owon, Korea) in the DBS group.

3. Micro-PET imaging

A. ^{18}F -FDG and micro-PET scanning

Long-term plastic metabolic images were obtained using ^{18}F -fluorodeoxyglucose (FDG) in micro-positron emission tomography (PET). ^{18}F -FDG was prepared using an ion beam application ^{18}F -FDG synthesis module. ^{18}F -FDG was used as a radiotracer to reveal brain glucose metabolism. After a 30 min adaptation period, ^{18}F -FDG was administered via the lateral tail vein, and 30 min in the cage was allowed for ^{18}F -FDG uptake. The rat was anesthetized by isoflurane and a micro-PET scanning image was obtained. Body temperature was maintained using a hot pad. Micro-PET imaging was performed for 30 min³³⁻³⁶.

B. Analysis of imaging

^{18}F -FDG micro PET images were reconstructed using the ordered subset expectation maximization (OSEM) algorithm with 10 iterations. Nominal

pixel size was $0.43 \times 0.43 \times 0.81 \text{ mm}^3$. For statistical analysis, only the brain regions within the ^{18}F -FDG micro-PET brain images were manually extracted. To generate the ^{18}F -FDG rat brain templates, baseline images were coregistered to the respective images and resliced with trilinear interpolation ($0.4 \times 0.4 \times 0.4 \text{ mm}^3$) using statistical parametric mapping (SPM5; <http://www.fil.ion.ucl.ac.uk/spm>). Individual images were averaged to generate a ^{18}F -FDG rat brain template. Then, it was normalized to a magnetic resonance imaging (MRI) template placed in stereotaxic space for accurate anatomical information³⁶. All images were normalized using the ^{18}F -FDG rat brain template. All individually normalized images were smoothed to increase the statistical power with an isotropic Gaussian kernel (2 mm full width at half maximum; FWHM). Voxel-based statistical analyses were carried out with statistical parametric mapping. Proportional scaling was used for global normalization. The statistical threshold was set at $P < 0.05$ (family-wise error correction) with an extent threshold of 100 contiguous voxels. T-value maps of results were overlaid on transverse views of the MRI template to define voxels that showed significant change. To analyze correlations between brain areas with significant metabolic changes, average glucose metabolism in each activated or deactivated brain region was calculated with all voxels within

1 mm at the Paxinos position of each region³². Pearson's correlation coefficients were calculated for regions of interest ($P < 0.01$, two-tailed).

4. Analysis of the analgesic effect of high-frequency DBS on neuropathic pain rats

A. Behavior tests

von Frey and acetone tests were performed to evoke neuropathic pain symptoms. Rats on top of a wire mesh grid in an acrylic cage (8 × 10 × 20 cm) were allowed free access to their paws. After 30 min of adaptation, an innocuous mechanical stimulation was applied with a *von Frey* filament (8 mN bending force) 10 times to the lateral edge of the ipsilateral hind paws to test mechanical allodynia. The total number of lifting the ipsilateral hind paw was counted.

The acetone test was performed to assay thermal cold allodynia, using a tube attached to a 1 ml syringe. After 30 min of adaptation, 100 μ l of acetone was sprayed with a syringe five times onto the lateral edge of the ipsilateral hind paw at 5-minute intervals. The total number of lifting the ipsilateral hind paw was counted.

B. Immunohistochemistry

Four weeks after induction of neuropathic pain, rats were anesthetized with pentobarbital sodium solution (50 mg / kg, i.p. injection) in phosphate-buffered saline (PBS) and intracardially perfused with 400 ml of normal saline and 300 ml of ice-cold 4 % paraformaldehyde in PBS (pH 7.4). The brain and lumbar spinal cord were exposed, removed, and post-fixed in the same fixative for one day at room temperature. Tissues were transferred to 30 % sucrose in PBS and immersed for 48 hours at 4 °C. Tissues were frozen in O.C.T. compound (Tissue-Tek, Sakura Fintek, Torrance, CA, USA) at -20 °C and 20 µm coronal sections were cut serially with a freezing microtome. Sections were incubated with 3 % normal goat serum for 2 hours to prevent nonspecific immunoreactivity. All sections were immunoreacted with primary polyclonal antibody anti-c-fos (1 : 200; Santa Cruz Biotechnology, Inc., Santa Cruz, CA, USA) or GAD65 (1 : 500; Millipore, Temecula, CA, USA), for 24 hours at 4 °C, and incubated in streptavidin-biotinylated peroxidase complex (Vector Laboratories Inc., Burlingame, CA, USA) for 2 hours at room temperature. All sections were rinsed with PBS and incubated with biotinylated goat anti-mouse IgG (1 : 1000; Vector Laboratories Inc., Burlingame, CA, USA) or biotinylated goat anti-rabbit IgG (1 : 1000; Molecular Probes, Eugene,

OR, USA) secondary antibody. Signal was amplified using avidin and biotinlated horseradish peroxidase using an Elite ABC Vectastatin Kit (Vector Laboratories Inc., Burlingame, CA, USA). Sections were rinsed in PBS and reacted with a solution containing 3,3'-diaminobenzidine tetrachloride dehydrate and cobalt chloride/nickel ammonium in 0.05 M Tris-HCl buffer (pH 7.2) at room temperature.

For florescence staining, sections were immunoreacted with a primary polyclonal antibody against GAD65 (1: 500; Millipore, Temecula, CA, USA) for 24 hours at 4 °C. Fluorescein isothiocyanate (FITC)-conjugated secondary antibody (1: 1000; Santa Cruz Biotechnology, Inc., Santa Cruz, CA, USA) was added to each section, and sections were incubated for 2 hours at room temperature in the dark. Sections were rinsed with PBS and mounted with mount solution (Vector Laboratories Inc., Burlingame, CA, USA) and cover slips.

C. Western blot

Rats were decapitated with a guillotine, and the prefrontal cortex, thalamus, and dorsal quadrant from L4 to L6 of the spinal cord (ipsilateral dorsal horn) were gathered. Samples were homogenized in lysis buffer (Intron, Korea) and centrifuged for 10 minutes at 12,000 rpm, and the

protein in the supernatant was measured by bicinchoninic acid protein assay reagent kit (Pierce, Rockford, IL, USA). Proteins were separated using 10 - 15 % sodium dodecyl sulfate polyacrylamide gel electrophoresis, incubated with antibodies to c-fos (1 : 200; Santa Cruz Biotechnology, Santa Inc., Santa Cruz, CA, USA), GAD65 (1 : 500; Millipore, Temecula, CA, USA), parvalbumin (1 : 1,000; Sigma, Saint Louis, MS, USA), or β -actin (1 : 1,000; Sigma, Saint Louis, MS, USA) followed by horse radish peroxidase (1 : 1,000; Serotec, Oxford, UK), and detected using an ECL system (Pierce, Rockford, IL, USA)^{37,38}. The intensity of each band was determined by an analysis system (Multi Gauge version 3.0, Fuji Photo Film Co. Japan).

5. Verification of the analgesic effect by introducing GAD65 into the spinal dorsal horn

A. Preparation of the rAAV2-GAD65

Recombinant adeno-associated virus (rAAV) serotype 2 was constructed and produced using a AAV-helper free system from Stratagene (Kirkland, WA, USA). pAAV2-JDK-GAD65 was generated by direct ligation of linearized pAAV-JDK vector predigested with *EcoRI* and GAD65 DNA

fragments digested with *EcoR*I from pAAV-GAD65. The pJDK plasmid was derived from the ACP plasmid³⁹ by replacing the backbone containing the AMP^R gene (PvuII fragment) with one containing the Kan^R gene (*Hing* II / *Xcm*I) from the pVAX1 plasmid (Invitrogen) using blunt ligation⁴⁰. rAAV2-GFP encodes enhanced green fluorescence protein (GFP) under the CMV promoter in the backbone of the pAAV2 vector (Stratagene). rAAVs were produced in 293T cells using the calcium phosphate method by triple-transfection of both pRepCap and pHelper with either pAAV2-GAD65 or pAAV2GFP. For large preparations of rAAVs, 293T cells in 10×10 cm dish were transfected and rAAVs in the cells liberated and purified by the SSCP method. Following dialysis against PBS (pH 7.4), rAAVs were stored in PBS containing 5 % glycerol at -80 °C. The number of total and infectious virus particles was estimated with an ELISA kit (Progen Inc., Heidelberg, Germany) or immunocytochemistry for GAD65 (Chemicon, CA, USA)⁴¹.

B. rAAVs injection in rats

Two weeks after inducing neuropathic pain in rats, under pentobarbital sodium anesthesia (50 mg / kg, i.p. injection) 3 µl of rAAV2s were injected into the left sciatic nerve through a glass micropipette connected to a

Hamilton syringe^{42,43}. Behavior tests were performed before and after rAAV injection.

C. Microdialysis

The amount of *in vivo* gamma-aminobutyric acid (GABA) release per dorsal horn of the spinal cord was determined by high performance liquid chromatography (HPLC) following microdialysis. Anesthetized rats under urethane (1.25mg / kg, ip injection) were mounted on a stereotaxic frame and the dorsal surface of vertebra T13 exposed and held immobilized on the horizontal plane with a spinal clamp. The dura was opened carefully and a microdialysis probe (CMA/11, Sweden) was inserted into the spinal dorsal horn. The probe was perfused with an artificial cerebrospinal fluid (CSF) of 145 mM NaCl, 2.7 mM KCl, 1.2 mM CaCl, 1.0 mM MgCl, and 2.0 mM NaHPO at pH 7.4. The flow rate was carefully controlled to 1.0 μ l per min using a CMA/102 pump (CMA/microdialysis, Sweden), before 30 μ l of sample was mixed with 60 μ l of working solution composed of 3 ml of O-phthaldialdehyde (OPA) stock solution (2.7 mg OPA in 1 ml of MeOH, 5 μ l of 2-mercaptoethanol, and 9 ml of 0.1 M sodium tetraborate) and 1 ml of sodium tetraborate.

D. HPLC analysis

A reverse-phase column (AccQ-Tag, 3.9×150 mm, Waters for amino acid analysis, Ireland) was used for separation. The mobile phase was 0.02 M sodium acetate buffer containing 30 % acetonitrile at pH 4.6. Peaks were detected at 30 °C with a flow rate of 0.7 ml / min using RF-10Ax1 (Shimazu Corp., Japan) at 340 nm excitation and 460 nm emission wavelengths.

6. Statistical analysis

ANOVA followed by LSD was applied as a post-hoc test at each time point for statistical analysis. An independent *t*-test was used for comparison between groups. $P < 0.05$ was considered statistically significant. Statistical analysis was performed by SPSS (version 11.5; SPSS Inc., Chicago, IL).

III. RESULTS

1. Inducing neuropathic pain in rats

For identification of induced neuropathic pain on rat, I performed *von Frey* tests for mechanical allodynia and acetone tests for cold allodynia. After 6 weeks, mechanical allodynia scores increased up to 9.07 ± 0.32 times per 10 stimuli ($P < 0.01$). Cold allodynia scores increased up to 4.47 ± 0.16 times per 5 stimuli after neuropathic pain induction (Figure 2).

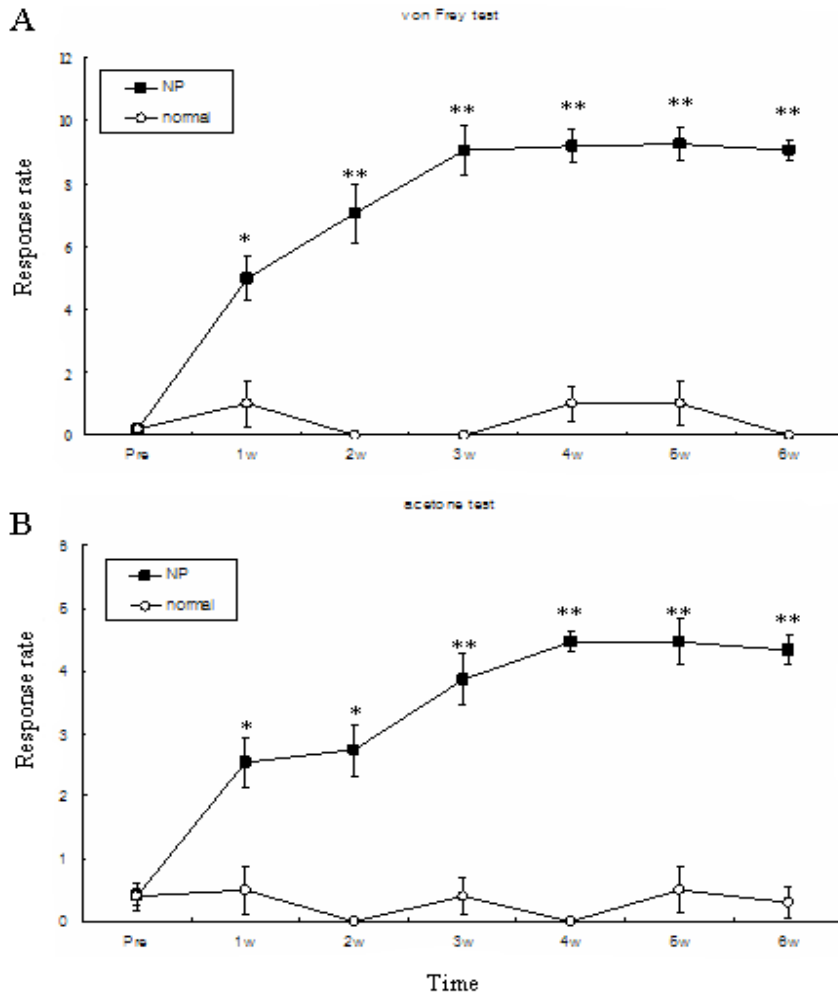


Figure 2. Comparison of behavior tests scores between neuropathic pain and naïve groups after sciatic nerve injury (A: mechanical allodynia test, B: cold allodynia test). (Pre: pre-operation, w: weeks since operation, NP: neuropathic pain group, normal: naïve group; * $P < 0.05$, ** $P < 0.01$)

2. Micro-PET scan of neuropathic pain rat models

To examine sequential changes in brain activation / deactivation in rats with induced neuropathic pain, micro-PET was performed at 2 and 4 weeks after pain induction. Micro-PET scanning values were plotted against time, for two independent groups, a naïve group (n=6), and a group in which neuropathic pain was induced (n=6).

The results showed that the amygdala and cerebellum were activated 2 weeks after induction of neuropathic pain and the radiatum layer of hippocampus was activated at 4 weeks after induction of neuropathic pain. However, the primary motor cortex and retrosplenial dysgranular cortex were deactivated at 2 weeks after pain induction and the retrosplenial dysgranular cortex was persistently deactivated until 4 weeks after pain induction (Figure 3).

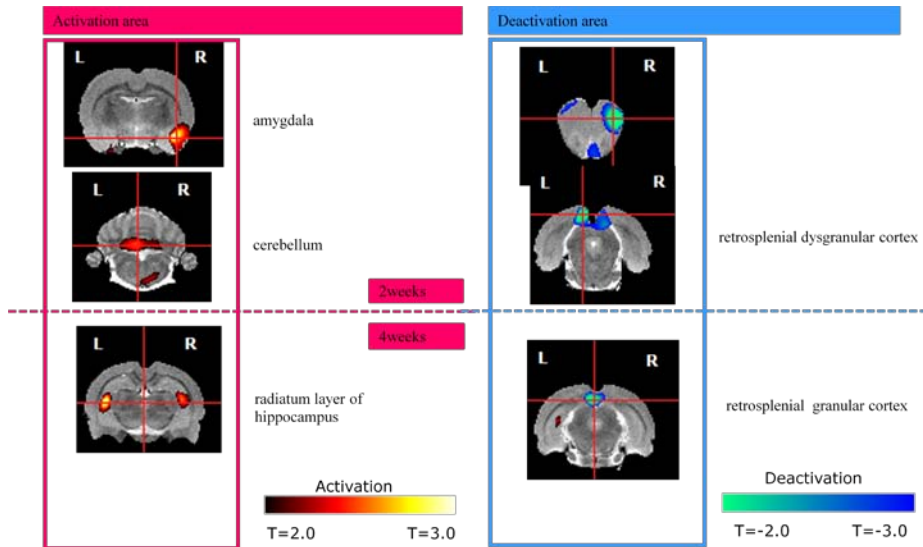


Figure 3. Activated (left) and deactivated (right) brain structures of neuropathic pain on rats. Brain activity images were obtained from neuropathic pain and naïve rats using micro PET.

3. Verification of the DBS electrode insertion effects

To examine the insertion effect of the tungsten stimulation electrode brain implant⁸, the frequency of foot withdrawals after repeated mechanical and cold stimuli was plotted against time for six independent groups: naïve rats (n=5), neuropathic pain-induced rat (n=5), neuropathic pain + ACC-implanted rats (n=10), neuropathic pain + PAG-implanted rats (n=10), neuropathic pain + VPM-implanted rats (n=10), and neuropathic pain + VPL-implanted rats (n=10). Few changes were noted for withdrawal of foot-lift in response to

mechanical and cold allodynia stimuli for all stimulation electrode-implanted groups compared to measurements before and after DBS (Figure 4).

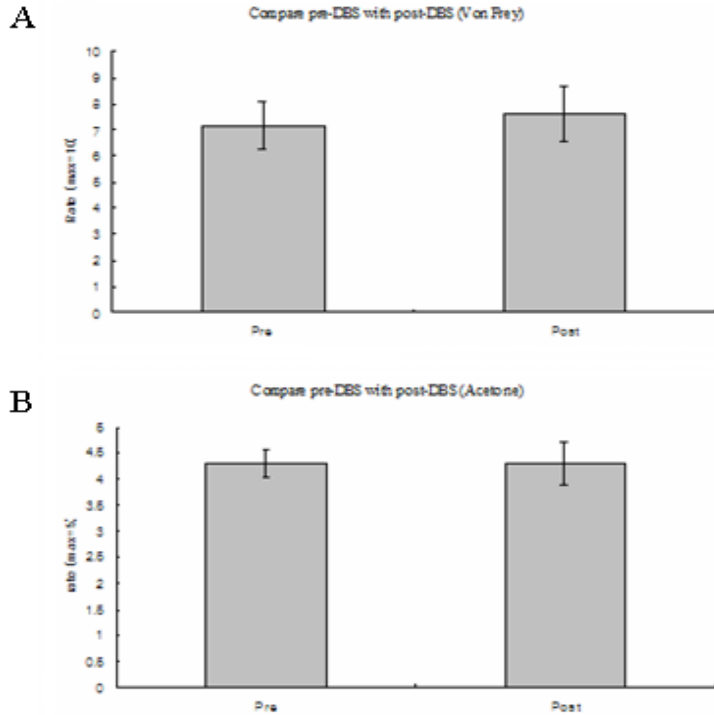


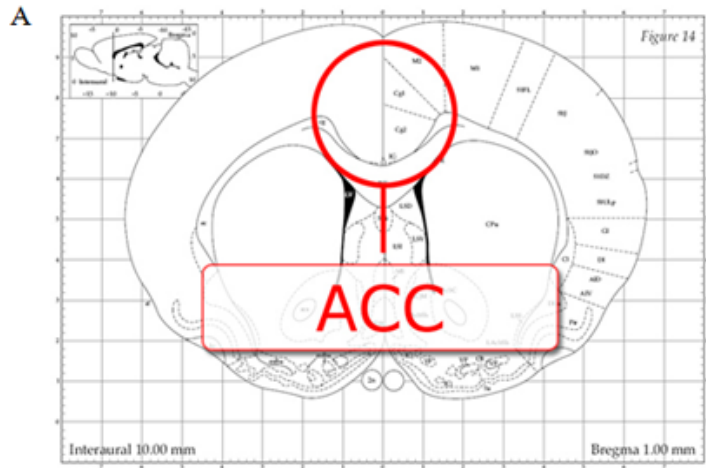
Figure 4. Withdrawal foot lift frequency at pre- and post-operation in DBS electrode implant groups. Pain response after DBS electrode insertion was the same as before DBS electrode insertion in mechanical (A) and cold allodynia tests (B).

4. Effect of high-frequency DBS according to target site

A. ACC

To investigate the analgesic effects of ACC-DBS, the DBS electrode was inserted into the ACC (n=10; Figure 5A), and *von Frey* and acetone behavior tests were performed. The stimulation parameters were 2 V, 130 Hz, and the duration was 60 μ s.

The withdrawal foot-lift in response to mechanical allodynia test slightly decreased during ACC electrical stimulation (Figure 5B), while the response to the cold allodynia test was unchanged during stimulation.



B

Mechanical allodynia

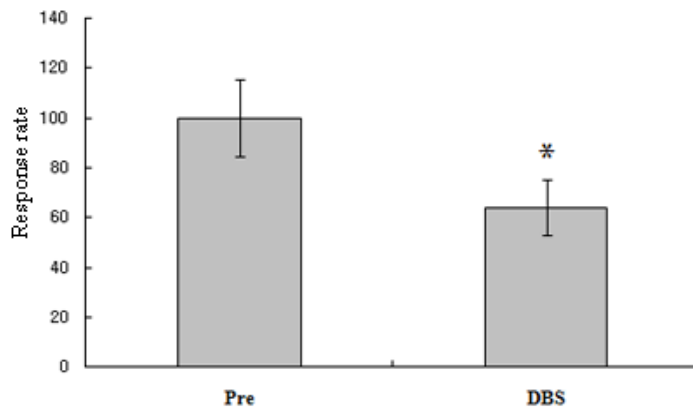


Figure 5. Target site of ACC and withdrawal foot-lift frequency for *von Frey* tests in neuropathic pain-DBS rats. ACC stimulation decreased withdrawal response compared to pre-stimulation in neuropathic pain rats. * $P < 0.05$. Pre means pre DBS state.

B. PAG

The effect of PAG-DBS on neuropathic pain-induced rats was blindly estimated by performing *von Frey* and acetone tests (Figure 6A). The frequency of withdrawal foot lift in response to repeated mechanical and cold stimuli slightly increased for both tests with PAG-DBS (Figure 6B, 6C).

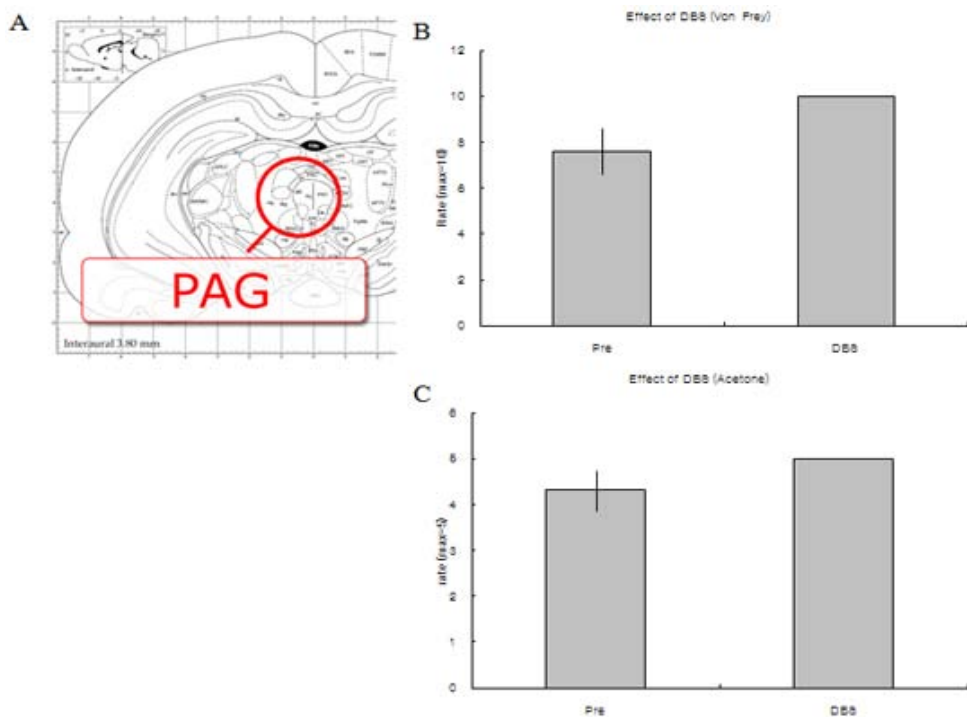


Figure 6. Behavior tests of mechanical and thermal allodynia for PAG-DBS in neuropathic pain rats before and after stimulation. Frequency of withdrawal foot lift in response to mechanical and cold allodynia increased slightly when

the DBS stimulator was turned on in experimental animals.

C. VPM

To investigate the analgesic effects of VPM-DBS in neuropathic pain-induced rats, electrodes were sited on the VPM (Figure 7A, 7B) and behavior tests performed as above. No analgesic effect was seen for cold allodynia with VPM-DBS in the neuropathic pain rat model, but was observed for mechanical allodynia (Figure 7C, 7D).

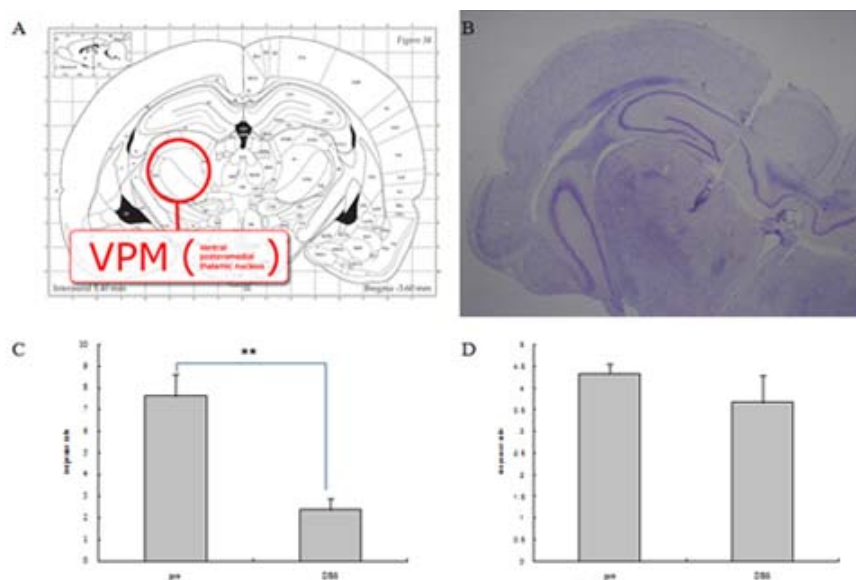


Figure 7. Mechanical and thermal allodynia before and after VPM-DBS in neuropathic pain rats. Asterisk (*) indicates that DBS in neuropathic pain rats differed significantly from the pre-DBS condition. ** $P < 0.01$.

D. VPL

Using the methods above, I investigated the analgesic effects of VPL-DBS, by inserting the DBS electrode into the VPL (Figure 8A, 8B) and performing behavior tests. The frequency of withdrawal foot lift in response to mechanical allodynia significantly decreased after DBS in rats with neuropathic pain. However, no response reduction was observed by the acetone test (Figure 8C, 8D).

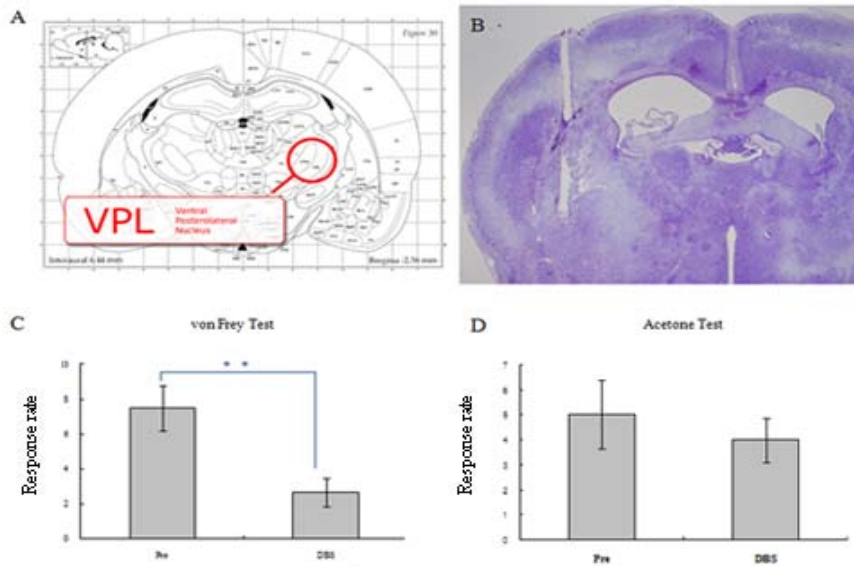


Figure 8. Mechanical and thermal allodynia before and after VPL-DBS in neuropathic pain rats. Asterisk (*) indicates that the response rate in VPM-DBS in neuropathic pain rats differed significantly from that in the pre-DBS condition. **P < 0.01.

5. Effect of DBS on c-fos, GAD65, and parvalbumin expression in brain and spinal dorsal horn

A. Effect of VPL-DBS in neuropathic pain rat

To examine c-fos expression in the spinal dorsal horn after VPL-DBS, rats suffering from neuropathic pain were prepared by inducing a peripheral nerve injury as described for pre-experiments. Two weeks after nerve injury, to verify the analgesic effect of VPL-DBS, DBS electrodes were implanted directly into the VPL of neuropathic pain-induced rat models (n=20) and naïve rats (n=5). Withdrawal foot-lift frequency by the *von Frey* test was counted blindly. The neuropathic pain + VPL-DBS group showed improvement from mechanical allodynia as expected (neuropathic pain: 9.4 ± 0.4 times per 10 stimuli, VPL-DBS: 3.6 ± 0.51 times per 10 stimuli). However, a DBS effect was not seen in the naïve + DBS group because of the low response rate to the *von Frey* test (Figure 9).

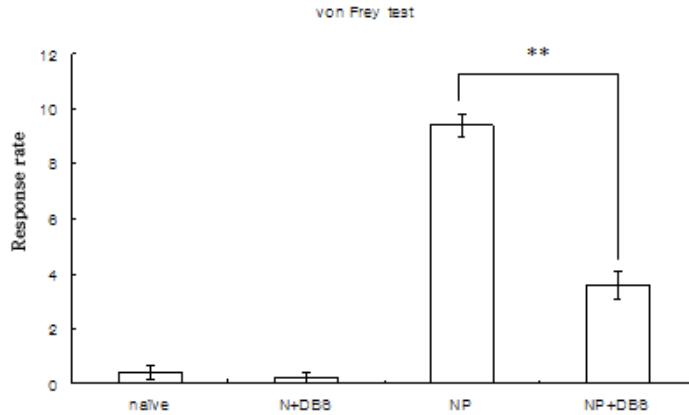


Figure 9. Mechanical allodynia of VPL-DBS. Frequency of withdrawal foot lift in response to *von Frey* tests were counted for naïve (naïve), naïve + DBS (N + DBS), neuropathic pain (NP), and neuropathic pain + DBS (NP + DBS) groups. Analgesic effect in neuropathic pain + DBS group was evident compared to the neuropathic pain group, but, the effect of DBS in naïve group was unclear because the frequency of withdrawal foot lift in *von Frey* tests was too low (** $P < 0.01$).

To investigate a plausible mechanism for the analgesic effect of DBS in rats with neuropathic pain, c-fos staining was performed on spinal dorsal horns. Figure 10 shows that c-fos expression decreased in the spinal dorsal horn after DBS in rats with induced neuropathic pain.

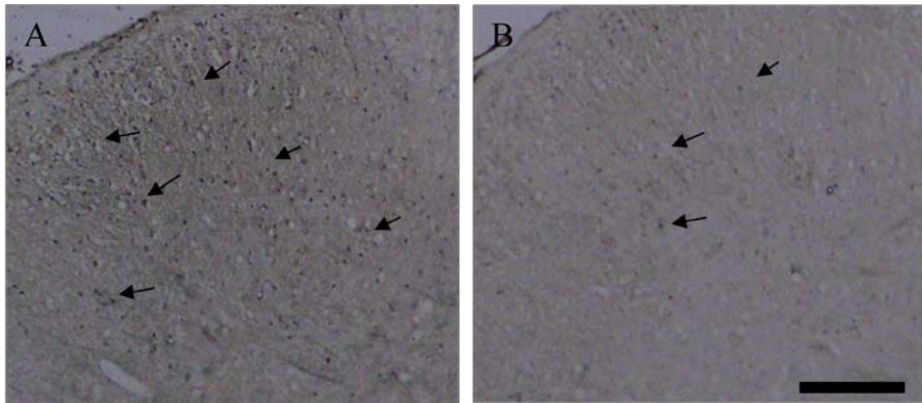


Figure 10. c-fos like immunoreactivity in neurons of the spinal dorsal horn in ipsilateral side (A: Neuropathic pain, B: neuropathic pain + DBS). Length of scale bar is 100 μ m.

B. Change of c-fos expression in the rat brain

To investigate changes in brain activation with VPL-DBS using the neuropathic pain rat model, western blots were carried out on prefrontal cortex and thalamus samples. Significant enhancement was seen in the level of c-fos expression in the prefrontal cortex, and a slightly increase was observed in the thalamus in the neuropathic pain stage in the rat model.

However, c-fos expression significantly increased after VPL-DBS in the neuropathic pain group in the prefrontal cortex. I also saw that c-fos expression in the thalamus was significantly increased after VPL-DBS compared to before VPL-DBS in the neuropathic pain rat model (Figure

11).

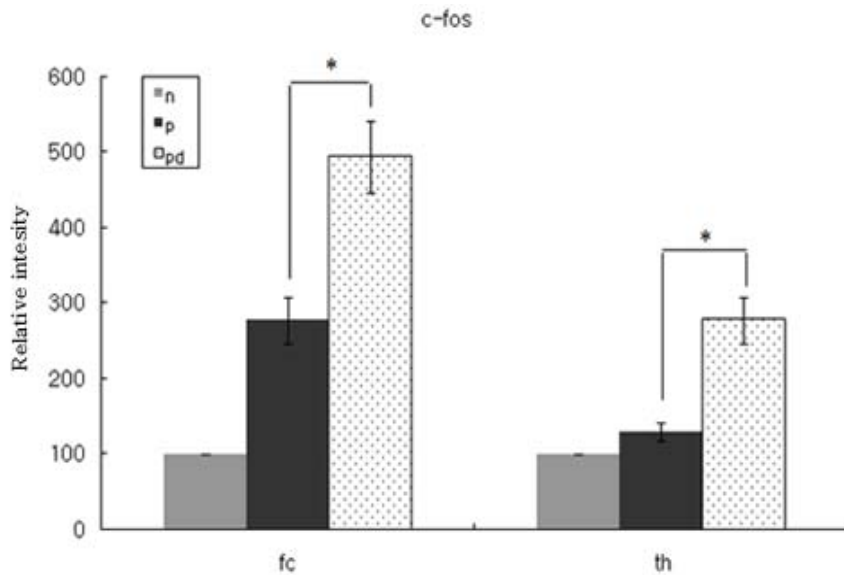


Figure 11. Comparison of c-fos expression among naïve (n), neuropathic pain (p), and neuropathic pain + DBS (pd) group in the prefrontal cortex (fc) and thalamus (th). Expression of c-fos in prefrontal cortex and thalamus significantly increased after VPL-DBS (* $P < 0.05$).

C. GAD65 immunoreactivity in spinal dorsal horn

Western blots were performed to examine GABAergic changes in spinal dorsal horn after VPL-DBS in the neuropathic pain rat model. GAD65 specific immunoblotting implied that GAD65 expression could be detected. The intensity of GAD65 expression with VPL-DBS was stronger in the

pre-DBS stage of the neuropathic pain rat model (Figure 12).

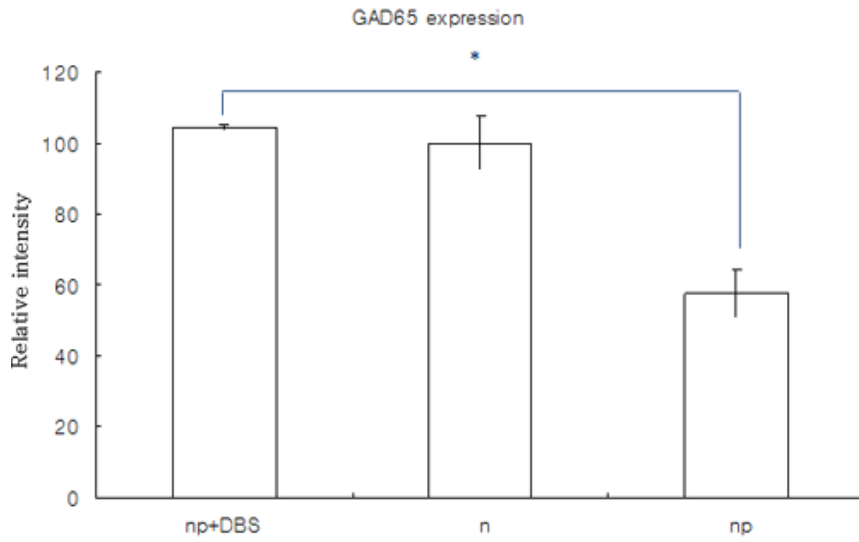


Figure 12. GAD65 expression in the ipsilateral spinal dorsal horn. Comparison was GAD65 expression among neuropathic pain + DBS (np + DBS), naïve (n) and neuropathic pain (np) groups in the spinal dorsal horn. Expression of GAD65 in neuropathic pain + DBS slightly increased compared to that in the neuropathic pain group (* P < 0.05).

D. Parvalbumin expression in spinal dorsal horn

Western blotting for parvalbumin was also performed to examine GABAergic neuronal changes in the spinal cord dorsal horn. The parvalbumin expression level increased after inducing neuropathic pain in

the spinal dorsal horn, so I observed parvalbumin for changes every week for 7 weeks after neuropathic pain induction. The level of parvalbumin expression increased after inducing neuropathic pain (Figure 13). Moreover, these changes were observed in the VPL-DBS group. These data showed that the parvalbumin expression level was not affected with VPL-DBS in the neuropathic pain rat model.

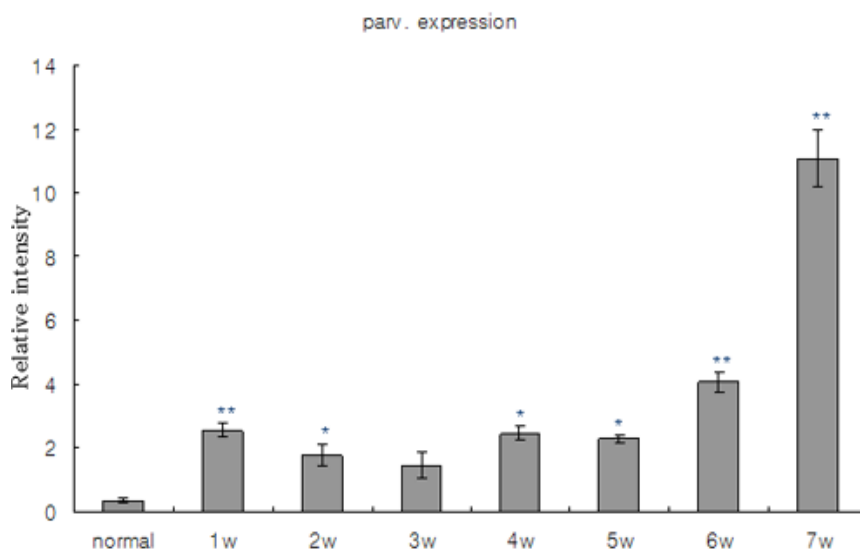


Figure 13. Parvalbumin expression in the spinal dorsal horn in neuropathic pain rats. Parvalbumin was measured by western blot from pre-surgery to 7 weeks after induction of neuropathic pain. Parvalbumin expression was significantly increased after induced neuropathic pain (* $P < 0.05$, ** $P < 0.01$).

6. Verification of analgesic effects by introducing GAD65 *in vivo*

A. rAAV expression GAD65 gene *in vitro*

rAAV vectors that expressed GAD65 or GFP genes were constructed. The wild type AAV2 virus has a terminal repeat sequence (TR) at each end of the genome with cap, rep, and polyadenylation sequence (poly A) genes. Viral plasmids were packaged using the AAV helper-free system⁴⁴, which uses iodixanol gradient ultracentrifugation for production and purification of a high titer of rAAV virus stock. By immunoblotting, GAD65 protein was detected in rAAV2-GAD65 infected HeLa cells, but no signal was seen for rAAV2-GFP infected cells (Figure 14).

To determine the expression of GAD65 or GABA *in vitro*, HeLa cells were coinfecting with rAAV2s and hAD5 at 5 MOI for 48 h, and analyzed by immunocytochemistry or immunofluorescence. The results suggested that rAAV-GAD65 was able to drive the production of GAD65 and GABA *in vitro* (Figure 15).

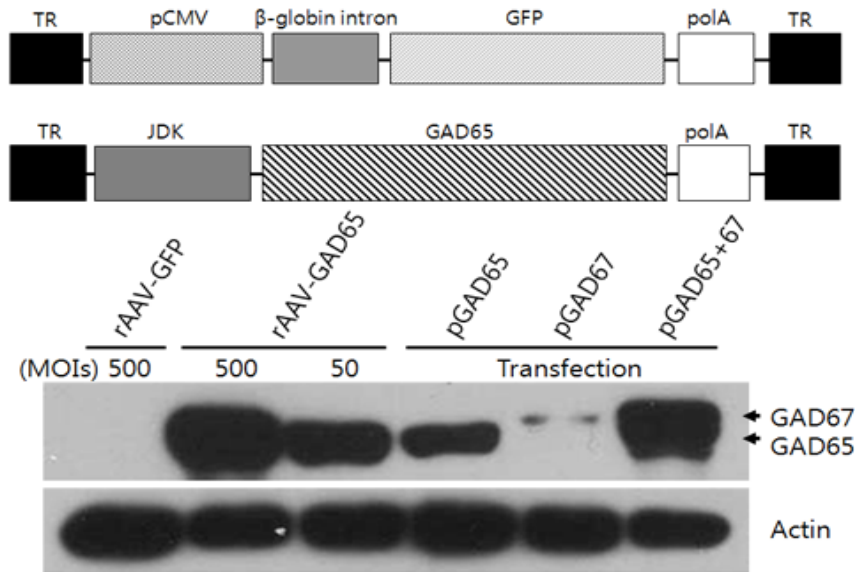


Figure 14. Schematic illustration of rAAV2 vectors and endogenous GAD65 expression in HeLa cells after transduction with rAAV vectors. All vectors contain the wild-type AAV2 TR sequence. Coding regions (GFP and GAD65), promoters (CMV, JDK), and poly A sequence are indicated.

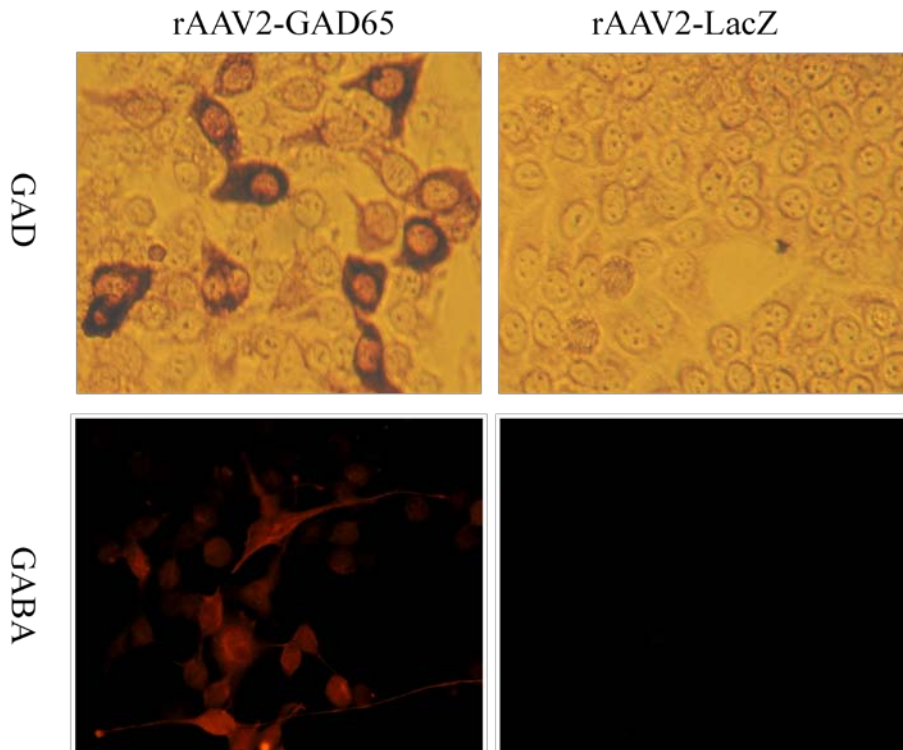


Figure 15. Detection of GAD65 and GABA expression. HeLa cells were seeded onto 48-well plates. After 24 hours, 10^5 total particles of rAAV2-GAD65 and rAAV-LacZ were applied to each well, and co-infected with hAD5 for 48 hours.

B. Injection of rAAV into the sciatic nerve efficiently transduced DRG in neuropathic pain rats

To investigate the transduction efficiency of rAAVs into dorsal root ganglia (DRG) through the sciatic nerve, GFP expression was monitored

after injection of rAAV2-GFP. Three μl of rAAV2-GFP (1.3×10^7 pfu / mL) was introduced into the sciatic nerve via glass electrode by injection ($n = 5$). rAAV2-GFP was observed in DRG neurons (Figure 16). These data showed that rAAV2 were strongly transduced to neurons in DRG. By expressing rAAV2-GFP in the control group for 3 weeks, the rAAV vector introduced via the sciatic nerve also moved to the DRG. Figure 16 shows that the L4 DRG became brightly fluorescent with GFP accumulation within 3 weeks after injection.

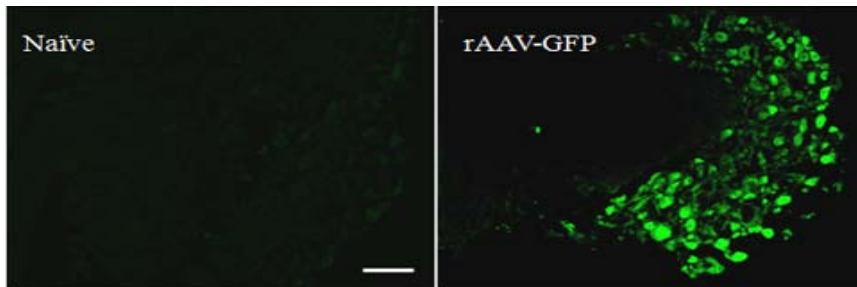


Figure 16. rAAV2-mediated transgene expression in DRG. After generating the neuropathic pain model, 3 μl of rAAV2-GFP (1.3×10^7 infectious particles / ml) were administered through the sciatic nerve using a glass micropipette. After 3 weeks, GFP expression in the L4 ipsilateral DRG was determined by fluorescence microscopy after cryo-sectioning. GFP expression was clearly detected in the rAAV2-GFP group, but not in the naïve group (original magnification: $\times 200$, scale

bar: 50 μm).

C. GAD65 can be detected by rAAV2-GAD65 injection into the sciatic nerve

Two weeks after inducing neuropathic pain in rats, 3 μl of rAAV2-GAD65 (6.2×10^7 / ml; infectious particles, n=6) and vehicle (n=5) were introduced into DRG neurons through the sciatic nerve, using a glass micropipette connected to a Hamilton syringe. Four weeks after injection, GAD65 transgene expression was detected in DRG neurons by immunohistochemistry using anti-GAD65 antibody. GAD65 decreases in groups in which neuropathic pain is induced, as seen by GAD65 immunohistochemistry⁴⁵. I found that GAD65 was present at the DRG using rAAV2-GAD65 that was injected through the sciatic nerve. The intensity of GAD65 expression in neuropathic pain-induced models with injection of rAAV2-GAD65 was significantly stronger than in vehicle injected models (Figure 17).

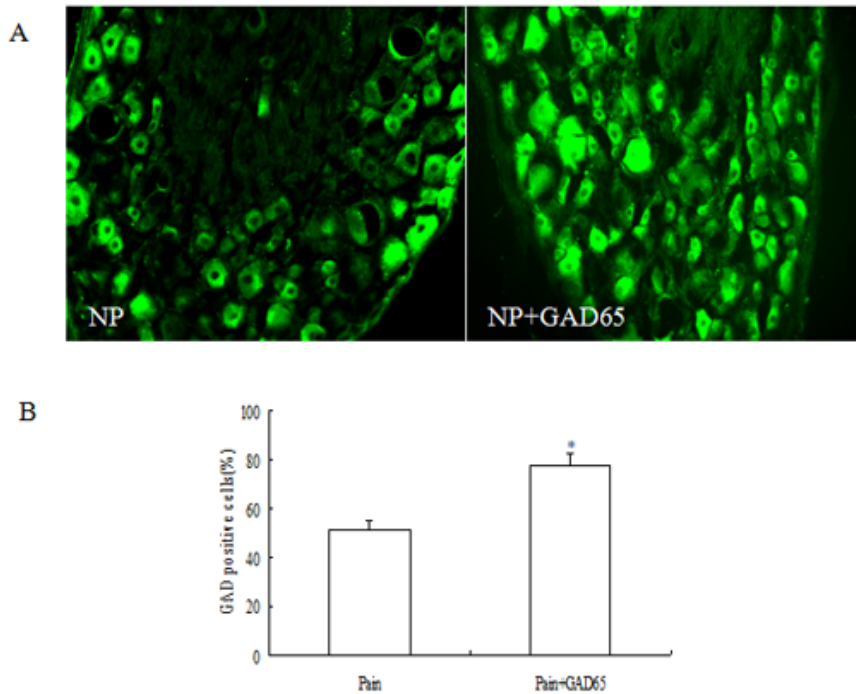


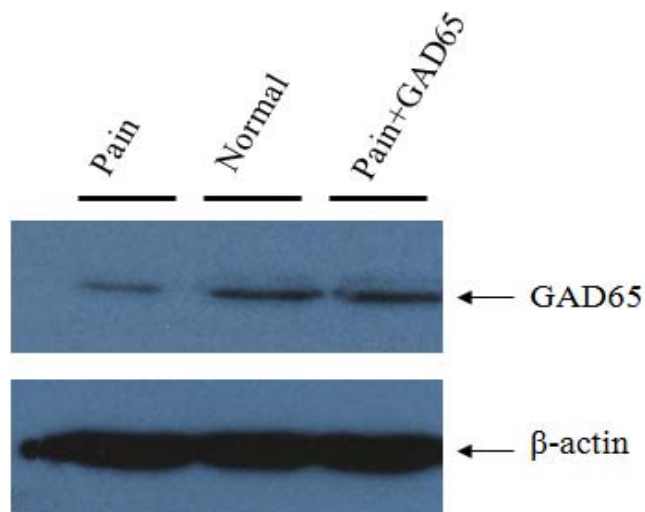
Figure 17. Expression of GAD65 in DRG. Immunohistochemical detection of GAD65 in the DRG after injection with rAAV2 vectors (A). Significant intensification of GAD65 expression was seen in the DRG pain model with rAAV2-GAD65 (B). Three μ l of rAAV2-GAD65 (6.2×10^7 /ml; infectious particles) were delivered to each L4 DRG through sciatic nerve injection (* $P < 0.05$; original magnification; $\times 200$).

D. Injection of rAAV2-GAD65 into the sciatic nerve produces GAD65 *in vivo*, induced by GABA increase in the spinal dorsal horn

To determine the level of GAD65, western blots showed a significant

decrease in GAD65 protein levels after sciatic nerve injury. In contrast, the rAAV2-GAD65-injected group showed more GAD65 protein level than the normal group (Figure 18).

HPLC analysis was carried out to determine whether GABA significantly increased in the dorsal horn following GAD65 expression in DRG. Four weeks after rAAV2-GAD65 inoculation into neuropathic pain-induced rats, *in vivo* GABA in the microdialysate of dorsal horns was determined by HPLC. The amount of GABA in the rAAV2-GAD65-injected group was 0.523 ± 0.033 pmol, which was substantially higher than the amount released in the saline-injected group (0.314 ± 0.065 pmol, Figure 19).



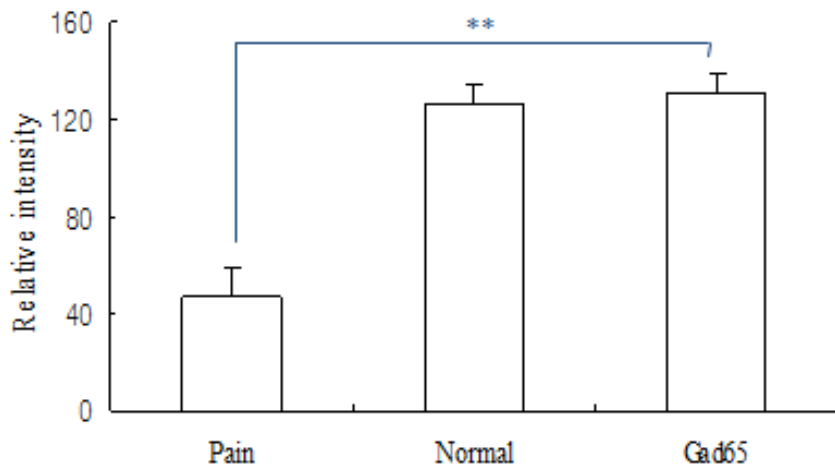


Figure 18. GAD expression in the spinal dorsal horn. Animals were sacrificed immediately after completing the final behavior tests; ipsilateral spinal dorsal horns were harvested and analyzed by western blot. A substantial increase in GAD expression was observed in the rAAV2-GAD65 administered group.

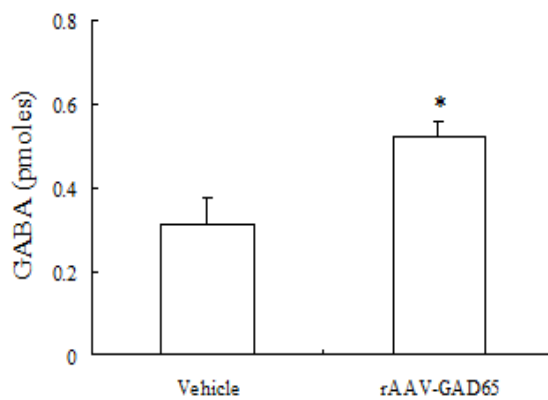


Figure 19. GABA secretion in the spinal

dorsal horn. GABA released from nerve terminals in the spinal dorsal horn was extracted *in vivo* from the CSF by microdialysis. The concentration of GABA in microdialysates was determined by HPLC seven weeks after surgery. GABA levels substantially increased in the rAAV2-GAD65 treated group compared to sham controls. (*P<0.05)

E. Injection of rAAV2-GAD65 reduces mechanical allodynia in neuropathic pain rat model

The beneficial effect from GAD65 synthesis in sciatic nerve injected with rAAV2-GAD65 was estimated blindly using *von Frey* testing for mechanical allodynia. Two weeks after surgery for induction of neuropathic pain, *von Frey* tests were used to measure the frequency of foot withdrawals with 10 mechanical stimuli event. Results were plotted against a final readout time from 4 independent groups that received either rAAV2-GAD65 (n = 6), or rAAV2-GFP (n = 5), or were control neuropathic pain (n = 7), and un-operated groups (naïve, n = 3) (Figure 20).

A week after rAAV2-vector inoculation, mechanical allodynia was significantly decreased in the rAAV2-GAD65 injected group compared to the neuropathic pain group. The rAAV2-GAD65-injected group showed continuous efficiency until the end of the experiment. No difference was observed in response to *von Frey* filament in control animals without surgery (naive group) over 8 weeks.

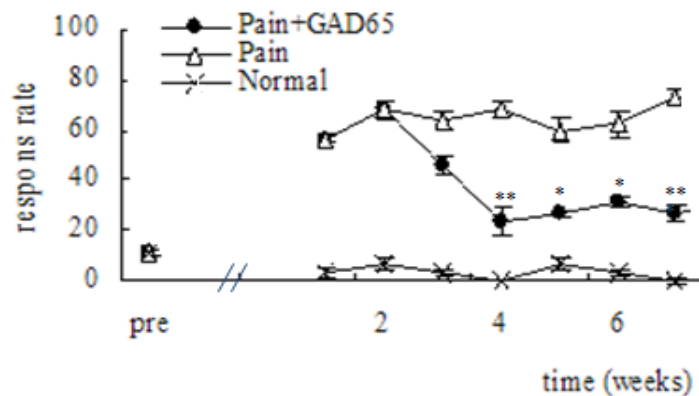


Figure 20. Therapeutic effects of sciatic nerve-administered rAAV2-GAD65 determined by behavior examination. Mechanical allodynia was assessed after virus administration in the neuropathic pain model by introducing 3 μ l of rAAV2 (1.3×10^7 infectious particles / ml). Asterisks indicate significant differences between the rAAV2-GAD65 group and the neuropathic pain group

(unoperated group (×), neuropathic pain group (△),
rAAV2-GAD65 injected neuropathic pain group (●),
*P<0.05, **P <0.01).

F. GAD65 reduces c-fos like immunoreactivity in spinal dorsal horn

Tibial and sural nerve transaction-induced expression of c-fos in the ipsilateral lumbar segment of the spinal cord was tested. c-fos like immunoreactivity neurons were quantified in the lumbar spinal laminae. Significant differences were observed between neuropathic pain group and rAAV2-GAD65 injected group at the ipsilateral side of the dorsal horn (Figure 21), but no significant difference was observed in the contralateral side for c-fos like immunoreactivity between them (data not shown). Normal and rAAV2-GAD65 injected groups were not significantly different in c-fos like immunoreactivity.

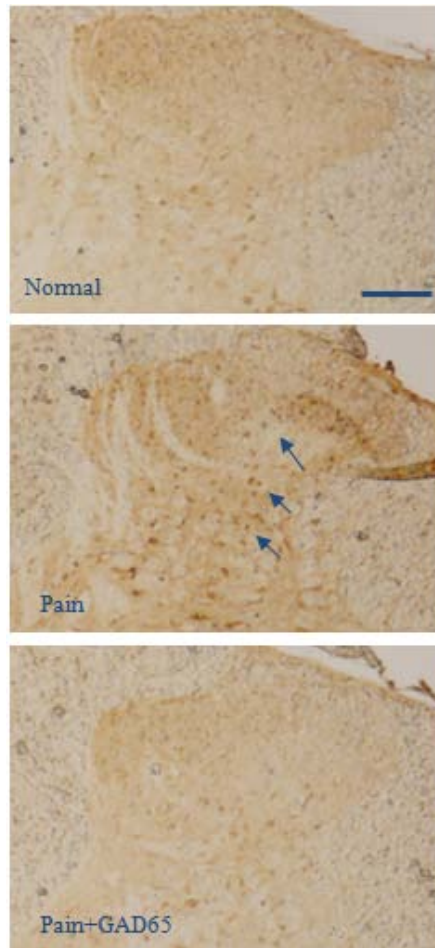


Figure 21. c-fos detection in the ipsilateral spinal dorsal horn. c-fos expression significantly decreased in the ipsilateral lumbar spinal cord of the rAAV2-GAD65 injected group (original magnification: $\times 200$; Scale bar: $100\ \mu\text{m}$).

IV. DISCUSSION

Neuropathic pain is a neurodegenerative chronic disease caused by lesions or dysfunction of diverse neural systems. It can be induced by multiple factors^{2,46}. Surgical treatment such as excision has been used traditionally^{6,47}, however, its effect is not always satisfactory because of invasiveness. In this study, DBS therapy was introduced via a less invasive method that did not cause side effects from tissue loss^{13,16}. DBS is widely used clinically, but the analgesic mechanism of DBS on neuropathic pain is not yet clearly known. Thus, this study was designed to determine how DBS exerts analgesic effects on symptoms in a neuropathic pain rat model. This study broadly followed three steps: establishment of a neuropathic pain rat model and DBS-implant surgery on the rats; confirmation of the analgesic effect of high-frequency DBS in the rat model and investigation of its effects; and verification of the analgesic effects by introducing GAD65 *in vivo*.

In the first step, neuropathic pain was induced by injury of the tibial and sural nerves, major divisions of the rat sciatic nerve²⁹ (Figure 1). This method produced stable responses to *von Frey* and acetone tests (Figure 2).

All DBS stimulation groups reduced pain score to mechanical allodynia after high-frequency DBS except the PAG region stimulation group. However,

clinical attempts and many studies suggest that PAG-DBS works well for neuropathic pain patients¹³. The results of these experiments were not consistent with previous descriptions because neuropathic pain has diverse causes and symptoms, and treatments differ by causes. Also the neuronal distribution of the human and rat brain is different, so stimulation sites might also be different⁴⁸. Recently, hyper-excitability within pain signaling neurons of the spinal cord dorsal horn and VPL nucleus was found to develop after traumatic nerve injury establishing a basis for central pain generators or amplifiers^{24,49,50}. High-frequency DBS of the nucleus suppresses neuronal activity²⁶. VPL-DBS was thought to reduce pain symptoms by suppressing neurons in the VPL hyperexcited by neuropathic pain, through the high stimulation frequency (130 Hz) used in this experiment.

The results are interesting because the analgesic effect in the allodynia behavior tests was seen only for mechanical, and not cold allodynia. Several groups have shown that the ACC, VPM, and thalamus increase activity during mechanical stimuli, but are not activated with cold stimuli, although insular is⁵¹. The domains involved in mechanical and thermal stimulation are suggested to exist at different regions of the nervous system⁵¹. Therefore, the stimulation site for these experiments could have been more affected by mechanical allodynia than by cold allodynia (Figure 22).

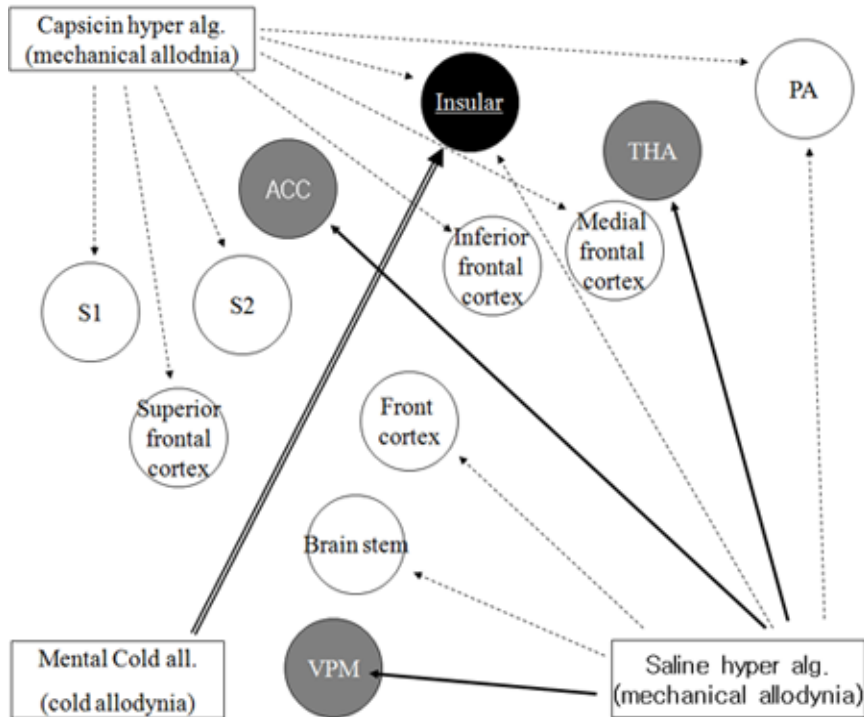


Figure 22. Activation of brain sites with mechanical and cold stimuli to neuropathic pain (S1: primary sensory cortex, S2: secondary sensory cortex, THA: thalamus, all: allodynia, alg: algisia).

Based on results of the first step, the second step was designed to implant stimulation electrodes into the VPL in the neuropathic pain group, to control neuropathic pain symptoms and investigate mechanisms of analgesia for VPL-DBS. Stimulation electrodes were implanted in a naïve + DBS group to investigate side effects and insertion effects from implantation of the

stimulation electrode and anchor system.

The prefrontal cortex and thalamus were analyzed by western blot with primary antibody against c-fos and the level of c-fos in the frontal cortex, thalamus increased³⁷. However, the level of c-fos in both the prefrontal cortex and thalamus area were significantly more increased after VPL-DBS in the neuropathic pain + DBS group than the neuropathic pain group(Figure 11). These results suggested that the VPL-DBS modulates neuropathic pain symptoms. Several studies suggested that c-fos may be a useful as a marker of neuronal activation following peripheral nerve injury^{37,52-54}. The thalamus controls the pain threshold and the prefrontal cortex area regulates the emotional aspects of chronic pain⁵⁵. A previous report showed that the prefrontal region acted as descending inhibitory controls for the pain threshold in patients treated with motor cortex stimulation (MCS)^{56,57}.

Subsequently, I analyzed the spinal dorsal horn by western blot with anti-GAD65 and anti-parvalbumin to investigate changes in the GABAergic system in the spinal dorsal horn. Quantitative analysis of immunoblotting results indicated that GAD65 expression decreased after induction of neuropathic pain compared to the naïve groups, as described previously⁴⁵. However, parvalbumin expression increased after neuropathic pain induction, and the expression level significantly increased with time (Figure 13). After

VPL-DBS, GAD65 expression increased more significantly than in the neuropathic pain group (Figure 12). However, the level of parvalbumin in the spinal dorsal horn under these conditions was not changed compared to the neuropathic pain group. Parvalbumin exists in a subpopulation of GABA containing neurons and it is a calcium binding protein^{58,59}. However, this result suggested that parvalbumin expression in the spinal dorsal horn was not associated with analgesia from VPL-DBS in a neuropathic pain rat model.

GABA is the product of GAD, and is a principal inhibitory neurotransmitter in the dorsal horn of the spinal cord with an important role in the ventral horn⁶⁰. Two isoforms of mammalian GAD encoded by two distinct genes have been identified⁶¹. GAD65 is present in a membrane-associated form in the synapses and is principally involved in producing synaptic GABA for vesicular release. In contrast, GAD67 is distributed throughout the cell body and is mainly responsible for the production of cytosolic GABA by releasing GABA through a non-vesicular mechanism^{62,63}. Several studies have suggested that GAD expression and allowing GABA production transiently attenuated neuropathic pain after spinal cord and peripheral nerve injury^{45,64}. GAD65 concentration is lower than GAD67 in the dorsal horn of rat pain models⁴⁵.

The third set of experiments was designed to determine whether an increase

in GAD65 expression in the spinal dorsal horn after the VPL-DBS reduced the pain symptoms in the neuropathic pain rat model.

Based on this hypothesis, rAAV2-GAD65 was transfected into the DRG through the sciatic nerve to increase GAD65 expression level in the spinal dorsal horn (Figure 18). The result showed that the GABA level increased via expression of rAAV2-GAD65 administered *in vivo* through the sciatic nerve (Figure 19), and the pain score decreased (Figure 20).

An electrophysiological study with the spinal dorsal horn of neuropathic pain rats reported that neuropathic pain rats showed hypersensitivity compared to normal rats⁴⁵. Previous report suggested that GABA levels declined significantly in all laminae of the ipsilateral dorsal horn in neuropathic pain rat models, which may reflect reduced GABAergic inhibition⁶⁵. Recent study found that GABAergic inhibition occurs via the selective GAD65 release from the spinal dorsal horn of a neuropathic pain rat model⁶⁶.

These findings may suggest that regulation of GAD65 levels in the spinal dorsal horn by VPL-DBS is sufficient to attenuate pain symptoms caused by peripheral nerve injury in rats (Figure 23).

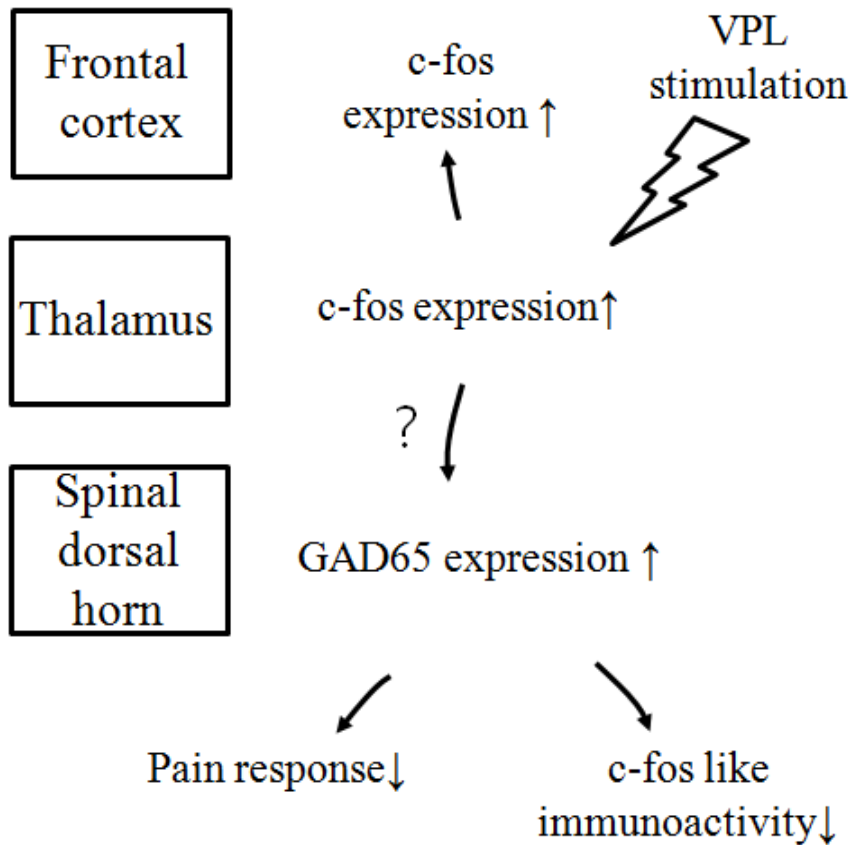


Figure 23. Molecular changes in the central and peripheral nervous system with VPL-DBS in the neuropathic pain rat model.

If so, the question was arose that how VPL-DBS could be affected the spinal cord. It could be proposed a hypothesis about the analgesic modulation of VPL-DBS in neuropathic pain rats. Stimulation of the thalamus activated on-, off- cells of the RVM. And then the spinal cord would be influenced through the activated off-cells.

The RVM is a major output of the endogenous modulatory system between the spinal cord and the brain⁶⁷. To explain hypothesis of the modulatory mechanism in detail, it can be supposed that the ② PAG and ③ spinal cord were affected consecutively by ① the DBS stimulation of the VPL, a part of the thalamus (Figure 24).

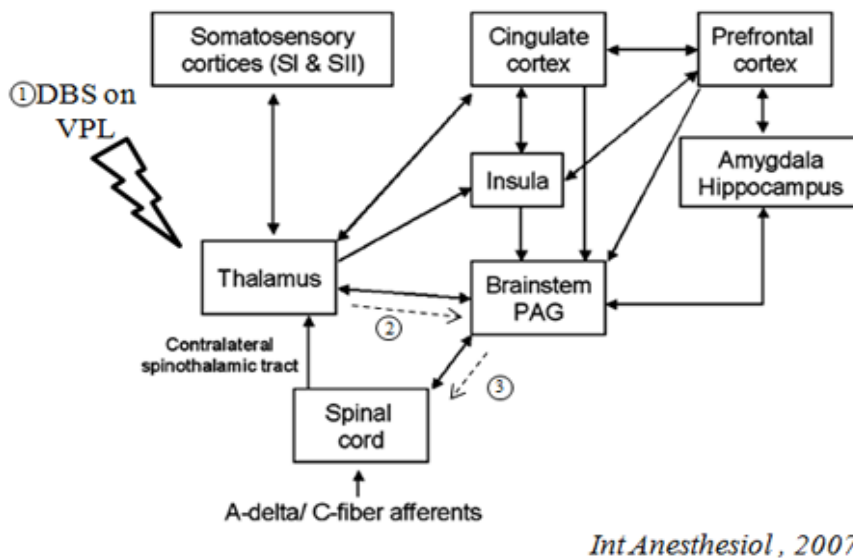


Figure 24. Descending modulation with VPL-DBS in the neuropathic pain rat model.

VPL-DBS gives electrical stimulation to the thalamus and influences PAG. PAG neurons, disinhibited by VPL-DBS, activate an opioid interneuron in the RVM and this endogenous opioid inhibits on-cells. The inhibition of on-cells

disinhibits off-cells, which inhibit nociceptive transmission at the level of the dorsal horn^{22,68,69} (Figure 25).

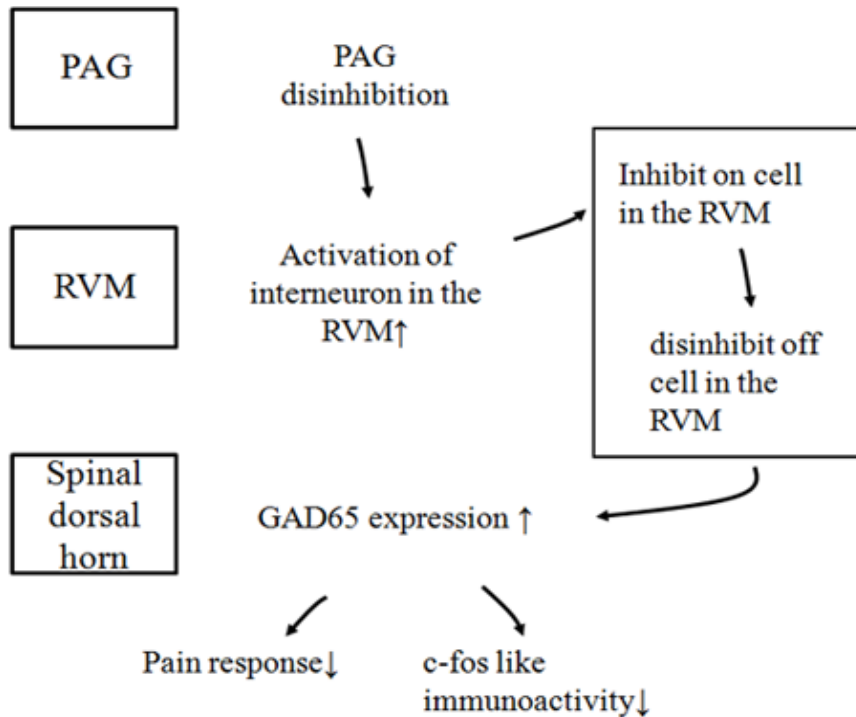


Figure 25. Hypothesis of descending modulation with VPL-DBS in the peripheral nervous system of the neuropathic pain rat model.

Through these processes, the effect of VPL-DBS may affect the spinal cord, attenuating pain symptoms.

V. CONCLUSION

Induction of sciatic nerve injury causes to change neuronal activation in the central and peripheral nervous systems. In addition, decrease in GABA levels in the spinal dorsal horn after peripheral nerve injury has been observed, suggesting that this change likely contributes to mechanical allodynia.

VPL-DBS in neuropathic pain rats reduced pain symptoms by: (1) high-frequency DBS stimulation, suppressing hyperexcitability neuronal signals in the thalamus in the VPL-DBS treated neuropathic pain group; (2) activation of the prefrontal cortex and thalamus to effectively regulate pain symptoms; and (3) stimulation to the thalamus affecting the spinal dorsal horn to upregulate GAD65 expression. Moreover, an increase in GAD65, the GABA-synthesizing enzyme, contributed to the dynamic changes in GABA expression in the spinal dorsal horn, leading to analgesia in the neuropathic pain rat model.

REFERENCES

1. Zhuo M. Neuronal mechanism for neuropathic pain. *Mol Pain* 2007;3:14.
2. Bridges D, Thompson SW, Rice AS. Mechanisms of neuropathic pain. *Br J Anaesth* 2001;87:12-26.
3. Woolf CJ, Mannion RJ. Neuropathic pain: aetiology, symptoms, mechanisms, and management. *Lancet* 1999;353:1959-64.
- 4.Coderre TJ, Katz J, Vaccarino AL, Melzack R. Contribution of central neuroplasticity to pathological pain: review of clinical and experimental evidence. *Pain* 1993;52:259-85.
5. Decosterd I, Woolf CJ. Spared nerve injury: an animal model of persistent peripheral neuropathic pain. *Pain* 2000;87:149-58.
6. Spooner J, Yu H, Kao C, Sillay K, Konrad P. Neuromodulation of the cingulum for neuropathic pain after spinal cord injury. Case report. *J Neurosurg* 2007;107:169-72.
7. Millan MJ. Descending control of pain. *Prog Neurobiol* 2002;66:355-474.
8. Hamani C, Schwalb JM, Rezai AR, Dostrovsky JO, Davis KD, Lozano AM. Deep brain stimulation for chronic neuropathic pain:

- long-term outcome and the incidence of insertional effect. *Pain* 2006;125:188-96.
9. Hocking G, Cousins MJ. Ketamine in chronic pain management: an evidence-based review. *Anesth Analg* 2003;97:1730-9.
 10. Yeng LT. [Pharmacological treatment of neuropathic pain]. *Drugs Today (Barc)* 2009;45 Suppl C:7-12.
 11. Shaladi AM, Saltari MR, Crestani F, Piva B. [Post-surgical neuropathic pain]. *Recenti Prog Med* 2009;100:371-9.
 12. Moro E, Lozano AM, Pollak P, Agid Y, Rehncrona S, Volkmann J, et al. Long-term results of a multicenter study on subthalamic and pallidal stimulation in Parkinson's disease. *Mov Disord* 2010.
 13. Bittar RG, Kar-Purkayastha I, Owen SL, Bear RE, Green A, Wang S, et al. Deep brain stimulation for pain relief: a meta-analysis. *J Clin Neurosci* 2005;12:515-9.
 14. Lozano AM, Snyder BJ. Deep brain stimulation for parkinsonian gait disorders. *J Neurol* 2008;255 Suppl 4:30-1.
 15. Johnson MD, Miocinovic S, McIntyre CC, Vitek JL. Mechanisms and targets of deep brain stimulation in movement disorders. *Neurotherapeutics* 2008;5:294-308.
 16. Rushton DN. Electrical stimulation in the treatment of pain. *Disabil*

Rehabil 2002;24:407-15.

17. Garcia-Larrea L, Peyron R, Mertens P, Gregoire MC, Lavenne F, Le Bars D, et al. Electrical stimulation of motor cortex for pain control: a combined PET-scan and electrophysiological study. *Pain* 1999;83:259-73.
18. Pereira EA, Green AL, Bradley KM, Soper N, Moir L, Stein JF, et al. Regional cerebral perfusion differences between periventricular grey, thalamic and dual target deep brain stimulation for chronic neuropathic pain. *Stereotact Funct Neurosurg* 2007;85:175-83.
19. Giummarra MJ, Gibson SJ, Georgiou-Karistianis N, Bradshaw JL. Central mechanisms in phantom limb perception: the past, present and future. *Brain Res Rev* 2007;54:219-32.
20. Zhao M, Wang JY, Jia H, Tang JS. Roles of different subtypes of opioid receptors in mediating the ventrolateral orbital cortex opioid-induced inhibition of mirror-neuropathic pain in the rat. *Neuroscience* 2007;144:1486-94.
21. Vanderah TW. Pathophysiology of pain. *Med Clin North Am* 2007;91:1-12.
22. Carlson JD, Maire JJ, Martenson ME, Heinricher MM. Sensitization of pain-modulating neurons in the rostral ventromedial medulla after

- peripheral nerve injury. *J Neurosci* 2007;27:13222-31.
23. Hubscher CH, Johnson RD. Chronic spinal cord injury induced changes in the responses of thalamic neurons. *Exp Neurol* 2006;197:177-88.
 24. Fischer TZ, Tan AM, Waxman SG. Thalamic neuron hyperexcitability and enlarged receptive fields in the STZ model of diabetic pain. *Brain Res* 2009;1268:154-61.
 25. Nishii H, Nomura M, Fujimoto N, Matsumoto T. Thalamic neural activation in the cyclophosphamide-induced visceral pain model in mice. *Neurosci Res* 2008;60:219-27.
 26. McCracken CB, Grace AA. High-frequency deep brain stimulation of the nucleus accumbens region suppresses neuronal activity and selectively modulates afferent drive in rat orbitofrontal cortex in vivo. *J Neurosci* 2007;27:12601-10.
 27. Anderson T, Hu B, Pittman Q, Kiss ZH. Mechanisms of deep brain stimulation: an intracellular study in rat thalamus. *J Physiol* 2004;559:301-13.
 28. Zimmermann M. Ethical guidelines for investigations of experimental pain in conscious animals. *Pain* 1983;16:109-10.
 29. Lee BH, Won R, Baik EJ, Lee SH, Moon CH. An animal model of

- neuropathic pain employing injury to the sciatic nerve branches. *Neuroreport* 2000;11:657-61.
30. Wu C, Wais M, Sheppy E, del Campo M, Zhang L. A glue-based, screw-free method for implantation of intra-cranial electrodes in young mice. *J Neurosci Methods* 2008;171:126-31.
 31. Bjornsson CS, Oh SJ, Al-Kofahi YA, Lim YJ, Smith KL, Turner JN, et al. Effects of insertion conditions on tissue strain and vascular damage during neuroprosthetic device insertion. *J Neural Eng* 2006;3:196-207.
 32. Paxinos G, Watson C. *The rat brain in stereotaxic coordinates*. 4th ed.: Academic Press; 1998.
 33. Fueger BJ, Czernin J, Hildebrandt I, Tran C, Halpern BS, Stout D, et al. Impact of animal handling on the results of 18F-FDG PET studies in mice. *J Nucl Med* 2006;47:999-1006.
 34. Shih YY, Chiang YC, Chen JC, Huang CH, Chen YY, Liu RS, et al. Brain nociceptive imaging in rats using (18)f-fluorodeoxyglucose small-animal positron emission tomography. *Neuroscience* 2008;155:1221-6.
 35. Maarrawi J, Peyron R, Mertens P, Costes N, Magnin M, Sindou M, et al. Differential brain opioid receptor availability in central and

- peripheral neuropathic pain. *Pain* 2007;127:183-94.
36. Ohashi K, Ichikawa K, Chen L, Callahan M, Zasadny K, Kurebayashi Y. MicroPET detection of regional brain activation induced by colonic distention in a rat model of visceral hypersensitivity. *J Vet Med Sci* 2008;70:43-9.
 37. Narita M, Ozaki S, Ise Y, Yajima Y, Suzuki T. Change in the expression of c-fos in the rat brain following sciatic nerve ligation. *Neurosci Lett* 2003;352:231-3.
 38. Kim J, Kim SJ, Lee H, Chang JW. Effective neuropathic pain relief through sciatic nerve administration of GAD65-expressing rAAV2. *Biochem Biophys Res Commun* 2009;388:73-8.
 39. Byun J, Heard JM, Huh JE, Park SJ, Jung EA, Jeong JO, et al. Efficient expression of the vascular endothelial growth factor gene in vitro and in vivo, using an adeno-associated virus vector. *J Mol Cell Cardiol* 2001;33:295-305.
 40. Jang HS, Kim HJ, Kim JM, Lee YS, Kim KL, Kim JA, et al. A novel ex vivo angiogenesis assay based on electroporation-mediated delivery of naked plasmid DNA to skeletal muscle. *Mol Ther* 2004;9:464-74.
 41. Lee B, Lee H, Nam YR, Oh JH, Cho YH, Chang JW. Enhanced

- expression of glutamate decarboxylase 65 improves symptoms of rat parkinsonian models. *Gene Ther* 2005;12:1215-22.
42. Gu Y, Xu Y, Li GW, Huang LY. Remote nerve injection of mu opioid receptor adeno-associated viral vector increases antinociception of intrathecal morphine. *J Pain* 2005;6:447-54.
43. Lee B, Kim J, Kim SJ, Lee H, Chang JW. Constitutive GABA expression via a recombinant adeno-associated virus consistently attenuates neuropathic pain. *Biochem Biophys Res Commun* 2007;357:971-6.
44. Hermens WT, ter Brake O, Dijkhuizen PA, Sonnemans MA, Grimm D, Kleinschmidt JA, et al. Purification of recombinant adeno-associated virus by iodixanol gradient ultracentrifugation allows rapid and reproducible preparation of vector stocks for gene transfer in the nervous system. *Hum Gene Ther* 1999;10:1885-91.
45. Moore KA, Kohno T, Karchewski LA, Scholz J, Baba H, Woolf CJ. Partial peripheral nerve injury promotes a selective loss of GABAergic inhibition in the superficial dorsal horn of the spinal cord. *J Neurosci* 2002;22:6724-31.
46. Campbell JN, Meyer RA. Mechanisms of neuropathic pain. *Neuron* 2006;52:77-92.

47. Francis DA, Christopher AT, Beasley BD. Conservative treatment of peripheral neuropathy and neuropathic pain. *Clin Podiatr Med Surg* 2006;23:509-30.
48. Kupers RC, Gybels JM. Electrical stimulation of the ventroposterolateral thalamic nucleus (VPL) reduces mechanical allodynia in a rat model of neuropathic pain. *Neurosci Lett* 1993;150:95-8.
49. Craner MJ, Klein JP, Renganathan M, Black JA, Waxman SG. Changes of sodium channel expression in experimental painful diabetic neuropathy. *Ann Neurol* 2002;52:786-92.
50. Zhao P, Waxman SG, Hains BC. Sodium channel expression in the ventral posterolateral nucleus of the thalamus after peripheral nerve injury. *Mol Pain* 2006;2:27.
51. Seifert F, Maihofner C. Central mechanisms of experimental and chronic neuropathic pain: findings from functional imaging studies. *Cell Mol Life Sci* 2009;66:375-90.
52. Nishimori T, Ikeda T, Terayama R, Ishida Y, Nakamura T, Otahara N. Effect of ionotropic glutamate receptor antagonists on Fos-like immunoreactivity in the dorsal horn following transection of the rat sciatic nerve. *Brain Res* 2002;934:81-6.

53. Tokunaga A, Kondo E, Fukuoka T, Miki K, Dai Y, Tsujino H, et al. Excitability of spinal cord and gracile nucleus neurons in rats with chronically injured sciatic nerve examined by c-fos expression. *Brain Res* 1999;847:321-31.
54. Herrera DG, Robertson HA. Activation of c-fos in the brain. *Prog Neurobiol* 1996;50:83-107.
55. Kishima H, Saitoh Y, Oshino S, Hosomi K, Ali M, Maruo T, et al. Modulation of neuronal activity after spinal cord stimulation for neuropathic pain; H(2)15O PET study. *Neuroimage* 2010;49:2564-9.
56. Kishima H, Saitoh Y, Osaki Y, Nishimura H, Kato A, Hatazawa J, et al. Motor cortex stimulation in patients with deafferentation pain: activation of the posterior insula and thalamus. *J Neurosurg* 2007;107:43-8.
57. Peyron R, Faillenot I, Mertens P, Laurent B, Garcia-Larrea L. Motor cortex stimulation in neuropathic pain. Correlations between analgesic effect and hemodynamic changes in the brain. A PET study. *Neuroimage* 2007;34:310-21.
58. Kawasaki H, Kretsinger RH. Calcium-binding proteins. 1: EF-hands. *Protein Profile* 1994;1:343-517.
59. Celio MR. Parvalbumin in most gamma-aminobutyric acid-containing

- neurons of the rat cerebral cortex. *Science* 1986;231:995-7.
60. Stoyanova, II. Gamma-aminobutyric acid immunostaining in trigeminal, nodose and spinal ganglia of the cat. *Acta Histochem* 2004;106:309-14.
 61. Erlander MG, Tillakaratne NJ, Feldblum S, Patel N, Tobin AJ. Two genes encode distinct glutamate decarboxylases. *Neuron* 1991;7:91-100.
 62. Feldblum S, Dumoulin A, Anoa M, Sandillon F, Privat A. Comparative distribution of GAD65 and GAD67 mRNAs and proteins in the rat spinal cord supports a differential regulation of these two glutamate decarboxylases in vivo. *J Neurosci Res* 1995;42:742-57.
 63. Soghomonian JJ, Martin DL. Two isoforms of glutamate decarboxylase: why? *Trends Pharmacol Sci* 1998;19:500-5.
 64. Hao S, Mata M, Wolfe D, Huang S, Glorioso JC, Fink DJ. Gene transfer of glutamic acid decarboxylase reduces neuropathic pain. *Ann Neurol* 2005;57:914-8.
 65. Eaton MJ, Plunkett JA, Karmally S, Martinez MA, Montanez K. Changes in GAD- and GABA- immunoreactivity in the spinal dorsal horn after peripheral nerve injury and promotion of recovery by

- lumbar transplant of immortalized serotonergic precursors. *J Chem Neuroanat* 1998;16:57-72.
66. Gwak YS, Crown ED, Unabia GC, Hulsebosch CE. Propentofylline attenuates allodynia, glial activation and modulates GABAergic tone after spinal cord injury in the rat. *Pain* 2008;138:410-22.
 67. Bee LA, Dickenson AH. Rostral ventromedial medulla control of spinal sensory processing in normal and pathophysiological states. *Neuroscience* 2007;147:786-93.
 68. Vazquez E, Escobar W, Ramirez K, Vanegas H. A nonopioid analgesic acts upon the PAG-RVM axis to reverse inflammatory hyperalgesia. *Eur J Neurosci* 2007;25:471-9.
 69. Morgan MM, Whittier KL, Hegarty DM, Aicher SA. Periaqueductal gray neurons project to spinally projecting GABAergic neurons in the rostral ventromedial medulla. *Pain* 2008;140:376-86.

ABSTRACT (IN KOREA)

신경병증성 통증 유발 쥐에서 심부뇌자극술의 효과

〈지도교수 장 진 우〉

연세대학교 대학원 의과학과

김 재 형

말초신경손상에 의한 신경병증성 통증은 임상에서 매우 일반적이다. 고주파의 심부뇌자극은 만성 신경병증성 통증에 효과적인 치료법으로 알려져 있다. 그러나 그것의 통증 완화 효과의 기전에 대해서는 아직 정확히 알려져 있지 않다. 고주파 심부뇌자극에 의한 신경병증성 통증 증상 완화 효과의 기전을 연구하기 위해, 말초신경을 손상시켜 신경병증성 통증을 유발시킨 수컷 흰쥐를 사용하였다. 쥐는 정상그룹, 정상 + 배쪽후외측핵-심부뇌자극 그룹, 신경병증성 통증 그룹, 신경병증성 통증+배쪽후외측핵-심부뇌자극 그룹의 4그룹으로 나눈다. 전전두엽, 시상, 척수 후각에서 배쪽후외측핵-

심부뇌자극의 전, 후의 변화를 c-fos 와 GAD65 의 단백질 검출 검사를 통해 검사하였다. 심부뇌자극술 후 신경병증성 통증 + 배쪽후외측핵-심부뇌자극 그룹에서 신경병증성 통증 그룹과 비교했을 때 통증 완화 효과가 나타났다. 그리고 배쪽후외측핵-심부뇌자극을 시행 후 전전두엽과 시상에서 급격한 c-fos 발현의 증가가 관찰되었다. 게다가, 신경병증성 통증+배쪽후외측핵-심부뇌자극 그룹에서 신경병증성 통증 그룹과 비교했을 때 척수 후각에서 GAD65의 발현이 증가되는 것을 단백질 검출 검사를 통해 관찰하였다. 반면에, 척수 후각에서 c-fos의 발현은 감소되는 것을 관찰하였다. 이러한 결과들로 보았을 때 배쪽후외측핵-심부뇌자극은 뇌와 척수에 영향을 미친다고 할 수 있다. 고주파 심부뇌자극은 과흥분된 신경 활성화, 특히 전전두엽과 시상부위의 신경활설도를 억제하고, 척수 등뿔에서의 GAD65의 발현을 증가시킴으로 통증 역치값을 조절한다.

핵심되는 말: 신경병증성 통증, 고주파 심부뇌자극술, 배쪽후외측핵, 글루탐산 카르복시 제거 효소, c-fos